https://ntrs.nasa.gov/search.jsp?R=19830005500 2020-03-21T05:19:08+00:00Z

General Disclaimer

One or more of the Following Statements may affect this Document

- This document has been reproduced from the best copy furnished by the organizational source. It is being released in the interest of making available as much information as possible.

- This document may contain data, which exceeds the sheet parameters. It was furnished in this condition by the organizational source and is the best copy available.

- This document may contain tone-on-tone or color graphs, charts and/or pictures, which have been reproduced in black and white.

- This document is paginated as submitted by the original source.

- Portions of this document are not fully legible due to the historical nature of some of the material. However, it is the best reproduction available from the original submission.

Produced by the NASA Center for Aerospace Information (CASI)

WHOI-82-48

Woods Hole Oceanographic Institution

DESCRIPTION AND EVALUATION OF THE ACOUSTIC PROFILING OF OCEAN CURRENTS (APOC) SYSTEM USED ON R.V. OCEANUS CRUISE 96 ON 11-22 MAY 1981

by

T. M. Joyce, S. R. Rintoul, Jr.,
and
R. L. Barbour

November 1982

TECHNICAL REPORT

Prepared for NASA under Grant NAG 1-91 through NASA-Langley

(NASA-CR-169529) DESCRIPTION AND EVALUATION OF THE ACOUSTIC PROFILING OF OCEAN CURRENTS (APOC) SYSTEM USED ON R. V. OCEANUS CRUISE 96 ON 11-22 MAY 1981 (Woods Hole Oceanographic Institution) 53 p

N83-13771

Unclas

G3/48 01148

WOODS HOLE, MASSACHUSETTS 02543

WHOI-82-48

DESCRIPTION AND EVALUATION OF THE ACOUSTIC PROFILING OF OCEAN CURRENTS (APOC) SYSTEM USED ON R.V. OCEANUS CRUISE 96 ON MAY 11-22 1981

by

T. M. Joyce, S. R. Rintoul, Jr.,
and
R. L. Barbour

WOODS HOLE OCEANOGRAPHIC INSTITUTION
Woods Hole, Massachusetts 02543

November 1982

TECHNICAL REPORT

Prepared for NASA under Grant NAG 1-91 through NASA-Langley.

Reproduction in whole or in part is permitted for any purpose of the United States Government.
This report should be cited as: Woods Hole Oceanog. Inst. Tech. Rept. WHOI-82-48.

Approved for Distribution: N. P. Fofonoff

N. P. Fofonoff, Chairman
Department of Physical Oceanography

TABLE OF CONTENTS

	Page
Abstract	1
Introduction	2
System Description	2
First Gulf Stream Crossing	6
Warm Core Ring Survey	9
Section Along 70°W	10
Intercomparison with a Moored Current Meter	11
Nantucket Shoals	12
Acknowledgements	14
References	15
Lists of Plates and Figures	16
Table	21
Plates 1 and 2	22
Figures 1 to 24	24

Abstract

The underway current profiling system used in this study consists of a microprocessor-controlled data logger that collects and formats data from a four-beam Ametek-Straza 300 kHz acoustic Doppler current profiler, heading from the ship's gyrocompass, and navigation information from a Loran-C receiver and a satellite navigation unit. Data are recorded on magnetic tape and some real time calculations are made. The system was first used on a May, 1981 cruise aboard the R.V. OCEANUS in the western North Atlantic. Horizontal currents were profiled to depths of 100 m. Time averaging is required to remove effects of ship motion. Errors in our ability to profile ocean currents are estimated to be 5-10 cm s^{-1} for a ten-minute vector average. An intercomparison is made with a moored vector measuring current meter (VMCM). The mean difference in hourly-averaged APOC and VMCM currents over the four-hour intercomparison is a few mm s^{-1}. Data from a variety of oceanic regimes are presented and discussed: these regimes include two Gulf Stream crossings, a warm core ring survey, and shallow water in a frontal zone to the east of Nantucket Shoals.

1. Introduction

By sensing the Doppler frequency shift between an outgoing and incoming acoustic pulse, the relative current between source and scatterer along the axis of the acoustic beam can be determined. Pinkel (1979) described an acoustic Doppler system and its application to the study of oceanic internal waves using the manned sparbuoy, FLIP, as a platform. If the oceanic scatterers, plankton, nekton, temperature microstructure or turbulence are assumed to be moving with the mean velocity of water, an ocean current profile as a function of acoustic range can be obtained from each back-scattered pulse. In what follows, a pulsed, 300 kHz, four-beam, acoustic transducer is hull-mounted and used to obtain vertical profiles of upper ocean currents relative to a ship whose lateral motion is determined by changes in LORAN-C position. The acoustic transducer and current profiling electronics, produced by Ametek-Straza (Rowe and Young, 1979), was installed on the R.V. OCEANUS and used on an eleven-day cruise, 11 to 22 May 1981 in the northwest Atlantic. We will describe the components of the profiler system and present some upper ocean current profiles obtained on the cruise. We have borrowed heavily upon an earlier system description (Joyce, Bitterman, Prada, 1982). In what follows, we will present results from two Gulf Stream crossings, a warm core ring survey, an intercomparison with a moored current meter in the Sargasso Sea, and data in shallow water to the east of Nantucket Shoals.

2. System Description

The Acoustic Profiling of Ocean Current (APOC) system consists of two main parts: the Ametek-Straza Doppler current profiler and a controller/data logger built at the Woods Hole Oceanographic Institution. The present system is shown schematically in Figure 1. From a transducer mounted in the hull of the ship, a 300 kHz acoustic pulse is transmitted in four beams down through the water column. As the acoustic signal travels through the water, it is scattered by small particles, temperature microstructure, or turbulence. By measuring the frequency of this return sig-

nal as a function of time or, equivalently, acoustic range, a profile of water velocity along the acoustic path can be obtained. Combining the data from the four beams with the ship's heading and subtracting out ship translation over the earth from navigation data yields a vertical profile of ocean currents. The method by which this is done is described later.

The 25.4 cm diameter transducer assembly has four 10 cm diameter flat plane acoustic radiators/receivers mounted at 30° angles to the vertical; two pairs of transducers define two orthogonal vertical planes. Each radiator transmits a 3° conical beam at 300 kHz. The beams can be approximately aligned in the fore, aft, port, and starboard directions relative to the ship. The four radiators are driven from one common 40-watt power amplifier that produces a sound pressure level of +225 db relative to 1 μPascal at a distance of one meter along each beam. Preamplifiers mounted in the transducer assembly amplify the return signals and send them via a shielded multiconductor cable to a second set of amplifiers before the signal processing stage. The transducer assembly also includes a thermistor temperature sensor to measure seawater temperature to compensate for sound speed variations due to temperature fluctuations. The transducer and adaptor parts used aboard OCEANUS are shown in Plates 1 (unassembled) and 2 (assembled).

Pulses of 300 kHz sound of 10 or 20 ms duration (pings) are emitted at regular intervals from the four radiators. The returned signal is detected by Ametek-Straza electronics. Following transmission of an acoustic pulse, the returned, amplified signal is detected in a frequency-locked loop whose frequency is measured in each of 31 time intervals. These intervals are switch-selectable for 5 or 10 milliseconds corresponding to vertical depth bins of 3.2 or 6.4 m allowing for the 30° beam angles from the vertical. The signal processor measures the amplitude of the return signal and sets a quality flag for each Doppler determination in which the signal strength is too low. Profile repetition is once every 1.2 seconds. The signal processors convert each good Doppler count to a 12-bit binary data word and a good-bad status bit for

each depth bin of each beam. Resolution of Doppler-induced currents for a single ping is 1.2 or 2.4 cm sec^{-1} depending upon the averaging time of 10 or 5 ms in the frequency-locked loop. A more detailed discussion of the detection electronics is given in Rowe and Young (1979).

To record information about the ship's heading and navigation, interface modules were built to convert data from the ship's gyrocompass, a Northstar 6000 LORAN-C receiver, and a Magnavox 706 satellite navigation receiver into a serial data stream that is transmitted over a 20-milliampere current loop. Each module is assigned a unique address and responds when the data controller sends out the proper address code. The current loop was selected because it requires only two simple wires to connect together modules located at various places on the ship. It also has a high level of noise immunity. Typically, this Serial ASCII Information Loop (SAIL) (Peal and Mellinger, 1981), transmits data at a rate of 2400 bits per second.

The controller/data logger is built around an 1802 type microprocessor having 4 k words of read-only memory for the operating program and 32 k words of random-access memory for temporary data formatting and storage. Data from 25 "pings" each with a ship's heading word are stored in memory to form a 30-second long data block. Navigation data, sea water temperature, and time of day from a precision clock are then added to the data record which is written onto a Kennedy Model 1600 nine-track digital tape recorder in IBM NRZI compatible format. This nine-track tape can be read for later processing. Typically, one 1200-foot tape is filled every eleven hours of operation. When the data are written onto tape they are also transmitted by the data logger to a small microcomputer which performs preliminary data conversion in real time for diagnostic purposes and a quick look at vector-averaged currents at selected depths.

For each pair of acoustic beams (Figure 2) the Doppler shift $\Delta\sigma_i$ can be written

$$\Delta\sigma_i = 2\, u_i \cdot k_i = 2\, |u_i||k_i| \cos(\theta_i - \phi_i) =$$

$$2\,\frac{\sigma}{c}\,(u_i \sin\phi_i + w_i \cos\phi_i), \quad i = 1, 2 \tag{1}$$

where σ is the acoustic frequency, c is the sound speed, and (u_i, w_i) are the components of the "scatterer" or ocean velocity in the vertical plane defined by the two beams. Thus, for each pair of Doppler measurements $\Delta\sigma_1$, $\Delta\sigma_2$, four unknowns remain (u_1, w_1), (u_2, w_2). The forward/aft looking "JANUS" arrangement with $\phi_1 = -\phi_2 = \phi$ allows a simple way out <u>if one assumes</u> the velocity vector to be the same at the two points 1, 2.

$$u = \frac{\Delta\sigma_1 - \Delta\sigma_2}{4\sigma}\,\frac{c}{\sin\phi}$$

$$w = \frac{\Delta\sigma_1 + \Delta\sigma_2}{4\sigma}\,\frac{c}{\cos\phi} \tag{2}$$

As the same argument can be made with the orthogonal pair, the horizontal velocity vector may be estimated along with two independent estimates of the vertical velocity. The difference in the two vertical velocities is therefore related to acoustic noise, imperfect estimation of Doppler shift and spatially variable currents. Near the ocean surface, the particle motions due to surface waves are greater, but the physical separation of the two ensonified regions is less. It is, therefore, not obvious which of the above factors dominates at any depth. Unlike the stable platform FLIP (Pinkel, 1979), ship motion due to surface waves is a signficant signal in the Doppler returns and must be considered. The instantaneous decomposition into fore/aft and athwartship velocities must be put into geographical coordinates because the ship is yawing as it pitches, heaves and rolls. This is done by measurement of the ship's heading for each data cycle. At the present time we are not trying to correct Doppler frequencies on a ping-by-ping basis to include components of wave-induced ship motion other than yaw; rather, we vector average the Doppler currents over many wave cycles and estimate lateral ship velocities from LORAN-C

data. Thus wave induced noise will be present, but it will be reduced by averaging over many wave cycles.

A significant source of error can be caused by misalignment of the acoustic transducer. If, instead of pointing fore, aft and athwartship the transducers are rotated a small angle α, then the forward motion of the ship through the water u_s, will cause a fore-aft, athwartship current errors proportional to u_s $(1-\cos \alpha)$, $u_s \sin \alpha$, respectively. For small α, this has little effect upon fore/aft currents, but it can cause large errors in attributing athwartship currents to the ocean when, in fact, they are due to the ship. This can be accounted for by steaming a steady course for 10-30 minutes then reversing direction noting that the ship-induced error changes sign. Further corrections can be made during processing once the offset is known. We note that for some applications it may be advisable to have the transducer assembly oriented so that all four beams avoid regions of any acoustic noise induced by the vessel such as air bubbles, which may, for example, degrade returns from the aft beam.

3. First Gulf Stream Crossing

The cruise track (Figure 3) shows an accented segment during which the Gulf Stream was crossed while the ship was on a southeast heading on 15 May. A ten-minute segment of raw Doppler counts for all 32 bins (31 data bins and one disabled bottom track bin) for each of the four beams is presented in Figure 4. It can be deduced from this ten-minute segment that ship's motion is a major source of noise in the system. In the port/starboard pair changes in ship attitude contribute to the 5-7 second period variance in the Doppler counts. Although data have been obtained down to 140 m, the percent of "good" data below 99 m (bin 16) is low. When the signal level is adjudged too low at the frequency detection stage, a quality bit is set and data from the last good range bin is inserted. Thus all deeper bins (higher bin numbers) change in concert; this is an artifact of the electronics and, merely signifies a low signal level. There is a second reason why the deeper bins will be changing in

concert even when the returning acoustic signals are large: no high-frequency surface wave currents penetrate to great depths. Thus, all variability in the Doppler returns is due to wave-induced platform motion, which is common to all range bins.

The dominant source of variability in the fore-aft pair is at periods on the order of one minute. This we believe is due to changes in the ship's forward speed. Periods of decreased Doppler in the fore beam coincide with increases in aft beam Doppler. This is especially noticeable at 0837Z and 0839Z in the figure. During this same ten-minute segment, the LORAN-C time delays have been plotted (Figure 5) between a master and three-slave pairs in the Northeast United States. LORAN-C Chain 9960 (U.S. Coast Guard, 1980). Stations W, X, Y are Caribou (Maine), Nantucket (Massachusetts) and Carolina Beach (North Carolina), respectively. A least-squares fit to a mean and slope is shown for each station pair. The present error in the slope estimation; based upon white noise assumption is 1-2 percent for the data shown. Since the ship was headed southeast at a speed of approximately 5 meters/sec, the error in constant ship speed is 5-10 cm sec^{-1}. At 0837Z in Figure 5, all three pair show a plateau in time delays. This could be due to a common error in the master station (Seneca, New York), but is more likely due to the slowing of the ship for a brief interval of time. Note that 0837Z is one of the times when the fore/aft pair of transducers (Figure 4) show a change of ship speed. The resolution of the Northstar 6000 LORAN-C is insufficient to detect subtle changes in ship speed, so without making further assumptions, this variability will degrade our ability to measure absolute current profiles to an accuracy 5-10 cm sec^{-1}.

Vector-averaged absolute currents have been calculated for ten-minute blocks of time for the Gulf Stream crossing accented in Figure 3 using "good" data for which the signal return is above a threshold value set by Ametek-Straza. Data from the transducer thermistor and vector currents at 28 and 99 meters (bins 5, 16) are shown along with an XBT section in Figure 6. The strong baroclinic signature of the Gulf Stream is between

XBT 101 and 105, a distance of about 90 km. Southeast of XBT 105, the warm surface core of the Gulf Stream is left behind and the thickening layer of 18° water, characteristic of the Northwest Sargasso Sea, is entered.

The thermistor temperature at a depth of 5 meters is constant through the warm core of the stream where currents are strongest, reaching speeds of 1.8 m s^{-1}. Currents in the Slope Water are westward, rapidly reversing at the north wall of the Gulf Stream where, at 0830Z, the front surfaces and vertical shears are large. At the southern edge of the warm core, the near-surface currents decrease in strength relative to those at 99 meters. Due to poor thermal contact between the thermistor in the Ametek-Straza transducer and seawater, there is a time lag of approximately 30 minutes between the thermistor and bucket samples.

Vertical profiles of horizontal currents for three selected ten-minute segments (see arrows in Figure 6) show the change in vertical structure across the section (Figure 7). The first profile, from the cold north wall, is calculated from the raw Doppler counts displayed in Figure 4. The current is predominantly eastward with a large amount of vertical shear and some rotation of the current vectors with increasing depth. In the second profile the eastward shear changes sign below 30 meters, probably a reflection of the geostrophic balance required by the presence of the warm, less dense core of the Gulf Stream. The Sargasso Sea profile has little vertical structure with predominantly weak northward flow into the axis of the Gulf Stream. For each of three profiles, the internal consistency of the relations (2) was tested by comparing the differences in vertical velocity in the fore/aft and athwartship acoustic pairs. The difference in the two "up" velocities is plotted on an expanded scale in the figure. Except at depths near 100 meters, where the paucity of "good" data in a 10-minute segment can become a problem, typical differences are 1-2 cm s^{-1}. This "error" ε, translates using (2) into estimates of errors in horizontal currents of $\pm\ \varepsilon\ \sqrt{3/2}$ or again, 1-2 cm s^{-1}. An intercomparison will be made in a later section with the moored current meter.

4. Warm Core Ring Survey

The cruise track for OCEANUS (Figure 8) shows a region south of Long Island on 14 May (year day 134) where a criss-cross pattern was made through warm core ring 80-G. Sea surface satellite images interpreted by the National Oceanographic and Atmospheric Administration (NOAA) and by the U.S. Navy had previously shown a warm core ring to be in this vicinity. A 34-hour mapping program was carried out as part of the oceanographic efforts on an eleven-day cruise. These legs of hourly XBT sections made by OCEANUS will be denoted by the run to the southwest (Leg 1), north (Leg 2) and the southeast (Leg 3). These are denoted by heavy lines on the cruise track.

The first leg (Figure 9a) revealed a gentle deepening of the isotherms with the greatest depression at XBT 68. Some isolated warm blobs of 13°C water were observed between 100-200 meters with considerable variability/ temperature inversions on either side of the deeper, warm core. A thicker homogeneous core of 13°C water was found on Leg 2 (Figure 9b) which deepened to nearly 400 meters on Leg 3 (Figure 9c) at XBT 88. Ring 80-G was an old ring probably formed during May of the previous year. During the course of the winter, cooling at the surface created a core of winter water within the center of the ring deeper than that in the surrounding Slope Water. The center of the ring, near XBT 88, was about 160 km northwest of the Gulf Stream, which OCEANUS approached beginning 0500Z on 15 May. Data from this crossing were discussed in the previous section. Surrounding the warm core, a number of cold inversions of 10°C water were found in the upper 50 meters.

A plan view of the deep temperature structure of the warm core ring was constructed using the deep expression of the 10°C isotherm depth. This represents the upper portion of the permanent pycnocline which is deep enough to escape the direct influence of wintertime cooling. Based upon this isotherm (Figure 10a) the center of the warm ring can be located near 38°20'N, 72°40'W. Surface salinities (10b) reveal the warm core

to be salty with values in excess of 35 practical salinity units. The data in Figures 10c,d were obtained from ten-minute averages from a four-beam, 300 kHz, Ametek-Straza velocity profiler which was equipped with a thermistor and mounted on the hull of the vessel at a depth of 5 meters. The horizontal currents displayed are for one vertical range cell of 6.4 meter thickness centered at 28 meters depth. A strong anticyclonic current pattern can be seen in Figure 10d around a ring center consistent with that revealed in 10a by the 10°C isotherm. Maximum swirl velocities of 50 cm sec^{-1} are found at a radius of 40-50 km from the ring center. Thus the core of the ring, were it in solid body rotation, would undergo a complete revolution once every six days. Outside of the ring of maximum swirl currents the velocity decreases and then increases to a secondary maximum. The position of this secondary maximum along Leg 3 coincides with an increase in slope of the 10° isotherm at XBT 96. Further steplike structure in the thermal field at XBTs 89 and 90 can be attributed to a two-hour time delay during which a CTD cast was made. The sharp decrease in slope between XBTs 90, 91 and 91, 92 may be a deeper signature of smaller scale structure within a warm core ring such as the secondary velocity maximum at a radius of 100 km from the ring center.

The vertical shear in the upper 100 m is small, and no attempt will be made to show its distribution. A single profile from the high velocity, inner core on Leg 3 (Figure 11), shows little structure; a likely result of the ring's over-wintering.

Results from this survey indicate that multiple maxima in the azimuthal velocity field can exist with increasing radial distance from the center of a warm core ring.

5. Section Along 70°W

On 19-21 May, OCEANUS steamed northward along 70°W taking hourly XBTs. A section from the Sargasso Sea to the Slope Water (Figure 12) of XBT data and 28 meter currents from the APOC system is shown in Figure 13. An elec-

trical storm caused interruption in the reception of Loran-C data on a portion of the section. As a result of the APOC data, it was surmised that OCEANUS passed to the west of a cold core ring which was centered near 34°N. This was supported by the XBT data. After the cruise an examination of the Ocean Frontal Analysis Charts produced from satellite VHRR infrared imagery was made which confirmed the existence of a cold core ring near 34°N,70°W. Note the strong confluence on either side of the Gulf Stream.

We do not record information about the amplitude of the Doppler returns in our Ametek-Straza transducer. A status bit is set, however, if the signal amplitude is below a fixed threshold value. This binary indicator of signal strength, when averaged over many returns (typically 500 in a ten-minute average) can be used as a qualitative indicator of the spatial variation in the scattering field. The percent return is plotted in Figure 14 along with surface temperature and velocity from the previous section. Doppler data are from 28 m depth and illustrate the "clear" warm core of the Gulf Stream in comparison with the Sargasso Sea to the south and the Slope Water to the north. These changes in signal amplitude return are presumably due to variations in zooplankton biomass, although no supporting evidence is available.

6. Intercomparison With a Moored Current Meter

Since the acoustic Doppler techniques are relatively new to the field of oceanography, it is important to gauge their success against the traditional techniques. A less than ideal, but nonetheless worthwhile, opportunity was offered on our May 1981 cruise aboard the OCEANUS (OC96) in which a comparison was made with a Vector Measuring Current Meter (VMCM) on a mooring of Mel Briscoe's at the site of his ONR-funded LOTUS surface mooring near 34°N,70°W. The VMCM was on a surface mooring at a depth of 36 m. For a period of 20 hours, the OCEANUS maintained station between this mooring and one containing a Profiling Current Meter (PCM) developed by Charles Eriksen and the MIT Draper Laboratories (1982). The water col-

umn at the time had little stratification and thus small vertical shear in the horizontal currents. Thus the comparison with PCM was not very fruitful. The VMCM functioned for only the first four hours of our "intercomparison" - between 1430-1830Z on year day 137. The ship track during this period (Figure 15) locates the OCEANUS midway between the two moorings, a distance of approximately 2 nm from the VMCM mooring. Note that the ship maintained position in a typically erratic fashion.

A time series of the APOC and VMCM currents (Figure 16) reveals a strong southward component to the current (we were, in fact, at the edge of a cold core ring) with a greater degree of "noise" in the 7.5 min APOC currents than the VMCM. Absolute currents from a moving ship are only as good as one's ability to monitor the ship motion. While steaming, this uncertainty in a 10-minute period gives rise to a 5-10 cm s^{-1} error in our ability to estimate a constant ship velocity from the half minute time series of LORAN position. While on station, this can be even noisier. The APOC system does provide accurate, unbiased currents, however, as can be seen in the table. The difference between hourly averaged VMCM and APOC currents yield means differences of only 0.3 and 0.2 cm s^{-1} with a standard deviation of 4.2 and 2.2 cm s^{-1} in the north and east components, respectively. We believe this agreement in the means to be as good as that which might be expected from two VMCMs moored 2 nm apart. The large standard deviation is a result of the erratic station keeping, and the shortcoming of our algorithm which assumes a constant ship velocity during the averaging interval (chosen to be ~ 7.5 min in Figure 16 to coincide with the VMCM sampling). A comparison of a vertical profile of APOC and PCM currents (Figure 17) made near 1613Z shows rather poor agreement. There was little shear in the water column at the time, but there appears to be an offset in current direction between the PCM and the APOC which at present remains unexplained.

7. Nantucket Shoals

The OCEANUS joined a group of NASA investigators taking part in the Nantucket Shoals Experiment (Wayne Esaisas, principal investigator). Dur-

ing an approximately 24-hour period between 11-12 May, we worked to the east of Nantucket Shoals near the site of a current meter mooring (A in Figure 18). For a ten-hour period we were hove to near buoy A. The currents from 20 m depth for this period show the strong semi-diurnal flow which dominates in the region (Figure 19). The mooring, which was set in 28 m of water depth was in a tidally-mixed zone to the west of a thermal front which ran parallel to the 70-m isobath. A survey of this thermal front over a tidal cycle (Figures 20-23) shows a strong thermal transition from cold, vertically-mixed water over the shoals to a stratified zone in deeper water. The 20-m currents along these transects are dominated (as in Figure 19) by a barotropic tidal signal. It is not possible to detect the signature of the thermal front in the current data without removing the tide. At this time, we were operating the APOC system with a 10 ms range gate window giving twice the vertical resolution supported in the results presented in earlier sections. A vertical profile of the currents near the large horizontal temperature gradient on Leg 2 at 1615Z (Figure 21) shows a southward current with a vertical shear (Figure 23) consistent with dynamical balance dominated by the "thermal wind" relationship associated with the front. We have no salinity data to make a quantitative comparison, however, and it is likely that baroclinic tidal velocities are contributing to the observed shear. We noted in a number of our vector-averaged profiles near the shoals a larger-than-average difference between the two vertical velocity estimates from the APOC system near the ocean surface(see right-hand side of Figure 24). As discussed in an earlier section of this report, this brings into question the accuracy of the horizontal velocities in the upper 15 m. Several possibilities for these larger errors (of more than 5 cm s^{-1}) might be suggested: side-lobe effects of the acoustic beams, inhomogeneities in the near-surface currents (possibly ship-induced), or the presence of strong turbulent patches which are not spatially coherent within the ensonified region. These differences together with our intercomparisons with a moored current meter in the previous section suggest that the acoustic technique used in APOC produces unbiased estimates of horizontal current but that caution should be exercised very near the ocean surface/ hull of the ship.

8. Acknowledgements

We gratefully acknowledge the cooperation of the captain and crew of the OCEANUS and Mel Briscoe, chief scientist of the cruise for help in obtaining these data. We are indebted to Briscoe for the use of his 70°W XBT data and the current meter data used in the intercomparison. We thank also Dave Bitterman who designed the APOC data logger and took part in the cruise, and Ken Prada for his advice and programming support. Lastly, we acknowledge the encouragement of Dr. Stan Wilson of NASA headquarters and the financial support of NASA Grant NAG 1-91 through NASA-Langley. Support for S. R. R. was provided through the WHOI Summer Student Fellow Program.

References

Eriksen, C. C., J. M. Dahlen and J. T. Shillingford, Jr. (1982). An upper ocean moored current and density profiler applied to winter conditions near Bermuda. Journal of Geophysical Research (accepted).

Joyce, T. M., D. S. Bitterman and K. E. Prada (1982). Shipboard acoustic profiling of upper ocean currents. Deep-Sea Research 29(7a): 903-913.

Peal, K. R. and E. C. Mellinger (1981). A standardized shipboard data acquisition system. IEEE Proceedings, Oceans 81: 287-291.

Pinkel, R. (1979). Observations of strongly non-linear internal motion in the open sea using a range-gated Doppler sonar. Journal of Physical Oceanography 9: 675-686.

Rowe, F. D. and J. W. Young (1979). An ocean current profiler using Doppler sonar. IEEE Proceedings, Oceans 79: 292-297.

U.S. COAST Guard (1980). Loran-C User Handbook. Department of Transportation Publication COMDTINST MI 6562.3.

List of Plates

Plates 1: Components of transducer and adaptor ring hardware for installation into the standard 10" transducer hole in pressurized chamber aboard R.V. OCEANUS.

Plate 2: Assembled transducer, associated hardware, and junction box. The latter was mounted in main lab of R.V. OCEANUS.

List of Figures

Figure 1: Schematic diagram of shipboard acoustic profiling system as configured during R. V. OCEANUS Cruise 96, 11 to 22 May, 1981.

Figure 2: Doppler geometry showing a pair of acoustic beams and scattering volumes moving with velocities u_1, u_2 at two equal acoustic ranges.

Figure 3: Ship track for R.V. OCEANUS Cruise 96, 11 to 22 May. After day 132 (May 12) 1200Z position of vessel is plotted. Heavy lines indicate XBT and current profiler section across the Gulf Stream.

Figure 4: Raw Doppler counts for four acoustic beams during a 10 minute period 0830-0840Z on day 135. An 1800-Hz range in the Doppler frequencies in the forward beam is used to scale the returns from each of the four beams.

Figure 5: Ten-minute series of time delays showing 30-s sampling for three stations in the northeast U.S. chain (9960) with least-square fits to a bias and slope for each time delay series.

Figure 6: Section across the Gulf Stream showing bucket (X) and thermistor temperatures (note the 30-minute lag of the thermistor), upper panel: vector-averaged currents at depths of 28 and 99 m (second and third panels, respectively); XBT section with XBT numbers and three 10-minute segments selected for current profiles and denoted by arrows.

Figure 7: Vector-averaged horizontal velocities for the three 10-minute time intervals shown in Figure 6 from the Gulf Stream north wall (●), south wall (▲), and Sargasso Sea (X). Difference between two vertical velocity estimates is plotted at the right on an expanded scale. Only data judged 'good' by Ametek-Straza interface cards were used. The large shear at 20 m in the north wall profile is across the base of the mixed layer and could be due to inertial waves.

Figure 8: Ship track for R.V. OCEANUS Cruise 96. Heavy line shows three XBT and current profiler sections through a Warm Core Gulf Stream Ring. The numbers identify each of the three sections.

Figure 9: Temperature profiles obtained from three XBT sections through the WCR. As numbered in Figure 8, Leg 1 is the upper panel (a), Leg 2 the second panel (b), Leg 3 the lower panel (c). All profiles are plotted as if the observer were looking from west to east. Numbers on the upper edge of each figure refer to XBT numbers; those on lower edge give temperatures at 760 m. Steep dipping of the isotherms at Stations 101 and 102 shows the beginning of the cold wall.

Figure 10a: The depth of the 10°C isotherm from XBT data showing the position of the ring center.

Figure 10b: Contour of surface salinities in the WCR from bucket samples at each XBT. Sharply increasing salinities south of the ring show the edge of the Gulf Stream.

Figure 10c: Contour of sea surface temperatures recorded by thermistor during ring crossing. Warm (15°-18°C) water at the SE and SW ends of the X-pattern shows the ship reached the cold wall of the Gulf Stream.

Figure 10d: Velocity vectors at 28 m depth in WCR calculated from 10-minute averages of the Doppler-velocimeter measurements. (◆) indicates 10-minute segment selected for current profile in Figure 11.

Figure 11: Vector-averaged horizontal velocities and temperature profile for 10-minute interval shown in Figure 10d. (Current record average begins at 2216 of day 134; temperature data from XBT 92, at 2200 of day 134.) Location of this profile is shown by the (◆) in the previous figure.

Figure 12: Ship track for R.V. OCEANUS Cruise 96. Heavy line denotes XBT and current profiler section along 70°W, from 33°N-40°N.

Figure 13: Section on 70°W showing vector-averaged currents at a depth of 28 m and XBT section with XBT numbers on the upper edge. (Electrical storm from 36°N to 37°N prevented accurate knowledge of ship motion, hence no velocity vectors could be calculated.)

Figure 14: Contour of surface temperature on 70°W section measured by thermistor (solid line) and XBT (X), upper panel; strength of return signal at 28 m expressed as fractional return, second panel. Velocity vectors at 28 m from Figure 13 are included in lower panel for comparison.

Figure 15: Ship track during intercomparison of current meters at the LOTUS site (see Figure 3). The position of the profiling current meter (PCM) and vector measuring current meter (VMCM) is indicated.

Figure 16: Time series comparison of velocity vectors obtained from VMCM at 36 m (Figure 16a) and APOC at 34 m (Figure 16b). VMCM values are recorded every 7.5 minutes; APOC values are 7.5 minutes (fourteen record) vector averages. (Unequal spacing of APOC vectors results from rounding off to the nearest minute in the calculation for average time.

Figure 17: Comparison of N and E components of horizontal velocity as measured by APOC, PCM and VMCM at approximately 1615Z day 137. (APOC profile is vector average of measurements made at 1607, 1614, 1622 and 1636Z; PCM profile made at 1613Z; VMCM value is average of observations between 1607 and 1633Z.)

Figure 18: Ship track for 11-12 May, over Nantucket Shoals, showing XBT positions (see Figure 3). Sections are identified by number; during each Doppler velocimeter operated continuously. A time series plot of velocity vectors at Buoy A (◆) is found in Figure 19.

Figure 19: Time series of 10-minute vector-averaged velocities at 20 m depth while on station at Buoy A (see Figure 18) from 0240-1100Z day 132.

Figure 20: Section 1 across a shallow thermal front on Nantucket Shoals showing surface temperatures from bucket samples (X), XBT (O), and thermistor (•), upper panel; vector-averaged currents at 20 m depth, second panel; temperature profile constructed from XBT data, including bottom topography, lower

panel. Dashed lines indicate half-degrees. Horizontal scale is the same in each figure.

Figure 21: Same as Figure 20 for Section 2 (see Figure 18), 15 km to the SE.

Figure 22: Same as Figure 20 for Section 3 (see Figure 18), repeating Section 1 six hours later.

Figure 23: Same as Figure 20 for Section 4 (see Figure 18), which repeats Section 2 six hours later.

Figure 24: Vector averaged horizontal velocity profile for the 10-minute interval 1623Z (see Figure 21).

Table: Comparison of hourly-averaged currents from APOC system (34 m) and moored VMCM (36 m) in ms^{-1}.

	VMCM		APOC		① − ②	
	N	E	N	E	N	E
1500	−.237	+.006	−.179	−.016	−.058	+.022
1600	−.247	−.011	−.238	−.020	−.009	+.009
1700	−.212	−.017	−.224	−.004	+.012	−.013
1800	−.191	.000	−.234	+.026	+.043	−.026
M	−.222	−.006	−.219	−.004	−.003	−.002
σ	.025	.010	.027	.021	.042	.022

ORIGINAL PAGE
BLACK AND WHITE PHOTOGRAPH

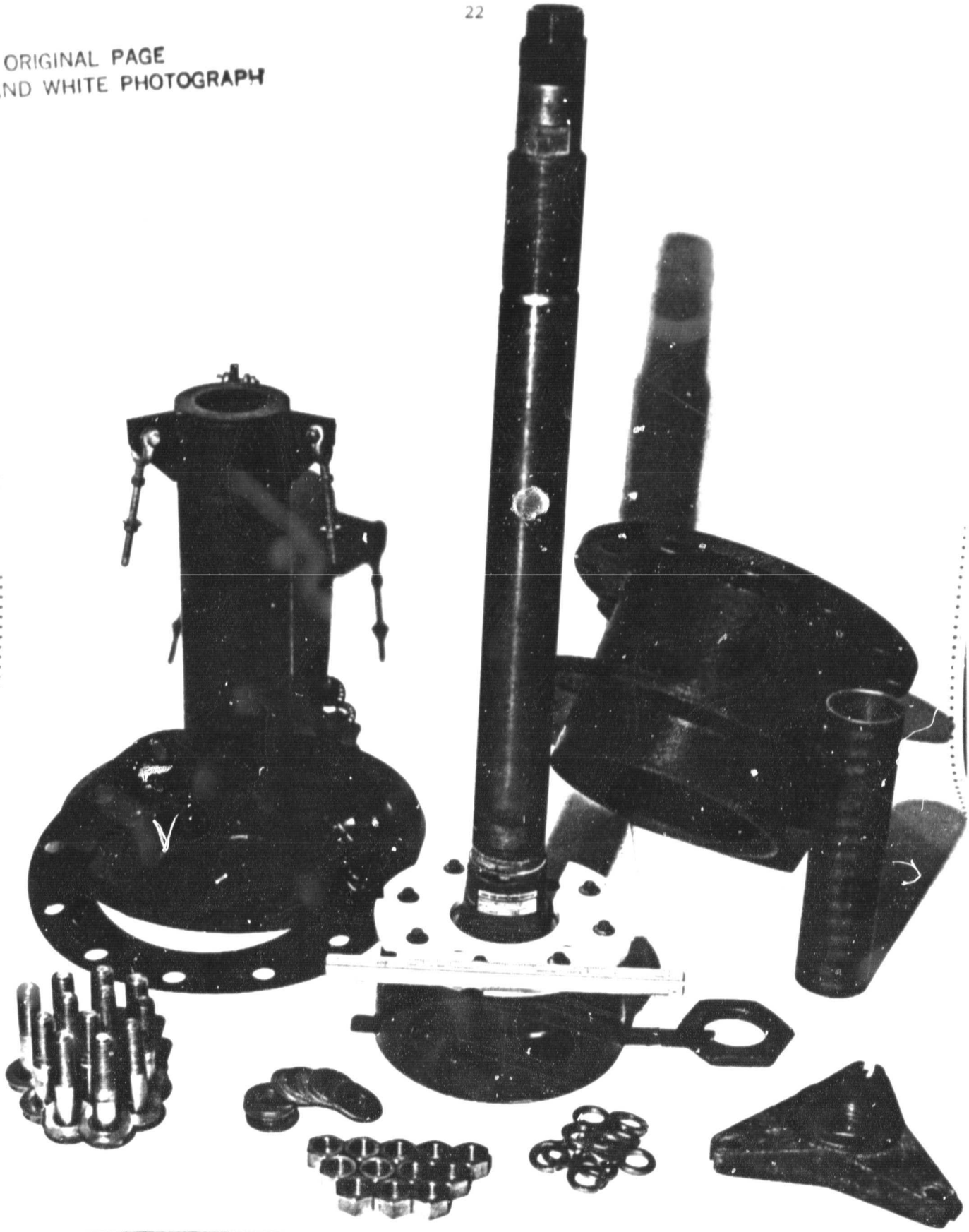

Plate 1: Components of transducer and adaptor ring hardware for installation into the standard 10" transducer hole in pressurized chamber aboard R.V. OCEANUS.

ORIGINAL PAGE
BLACK AND WHITE PHOTOGRAPH

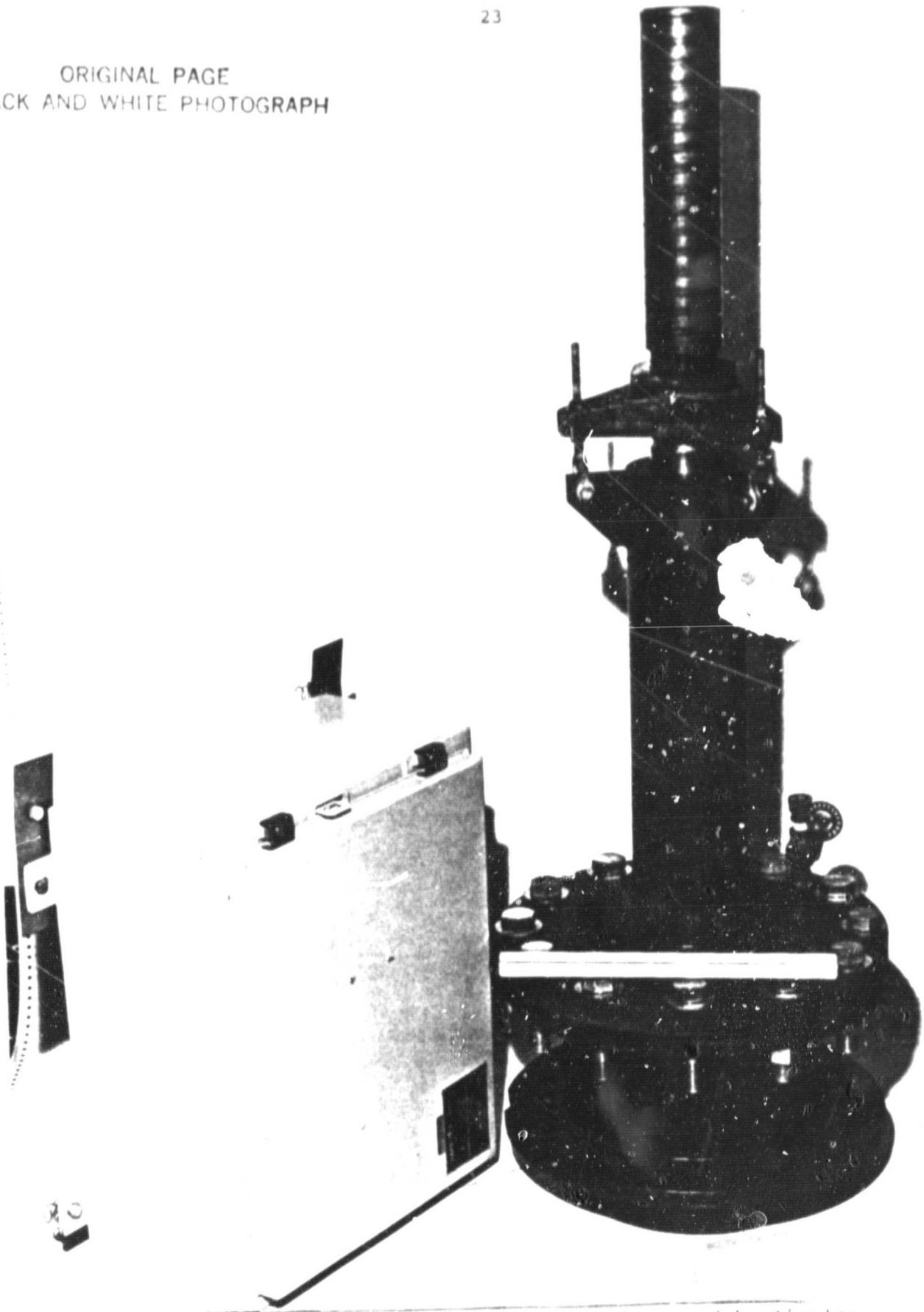

Plate 2: Assembled transducer, associated hardware, and junction box. The latter was mounted in main lab of R.V. OCEANUS.

ORIGINAL PAGE IS
OF POOR QUALITY

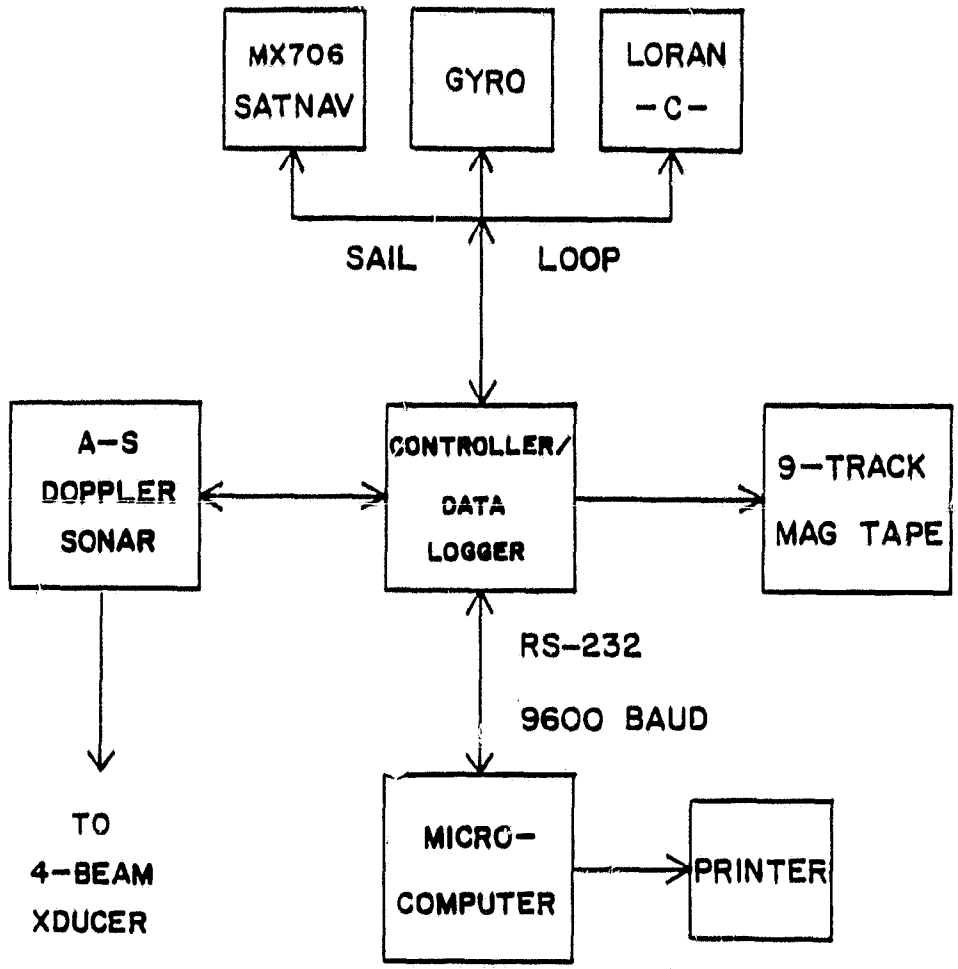

Figure 1: Schematic diagram of shipboard acoustic profiling system as configured during R. V. OCEANUS Cruise 96, 11 to 22 May, 1981.

ORIGINAL PAGE IS
OF POOR QUALITY

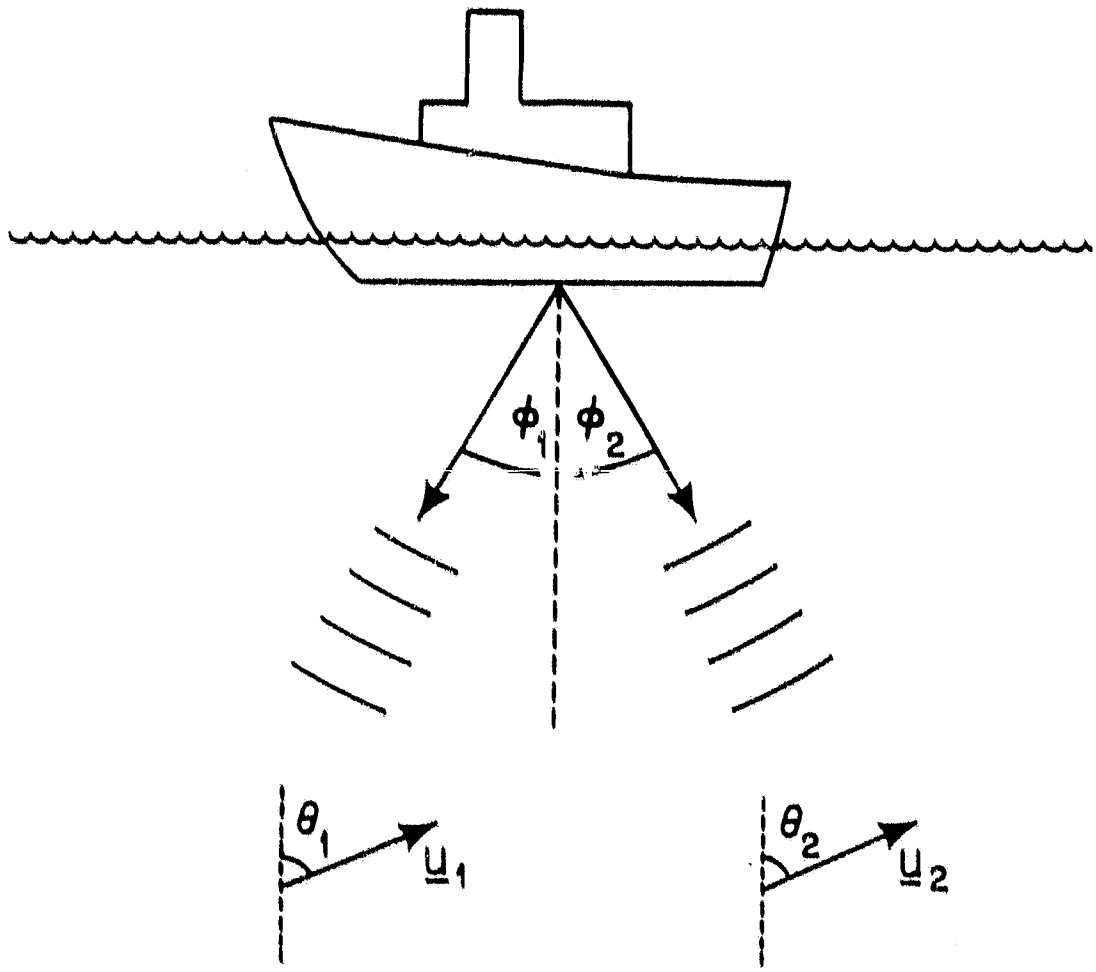

Figure 2: Doppler geometry showing a pair of acoustic beams and scattering volumes moving with velocities u_1, u_2 at two equal acoustic ranges.

ORIGINAL PAGE IS
OF POOR QUALITY

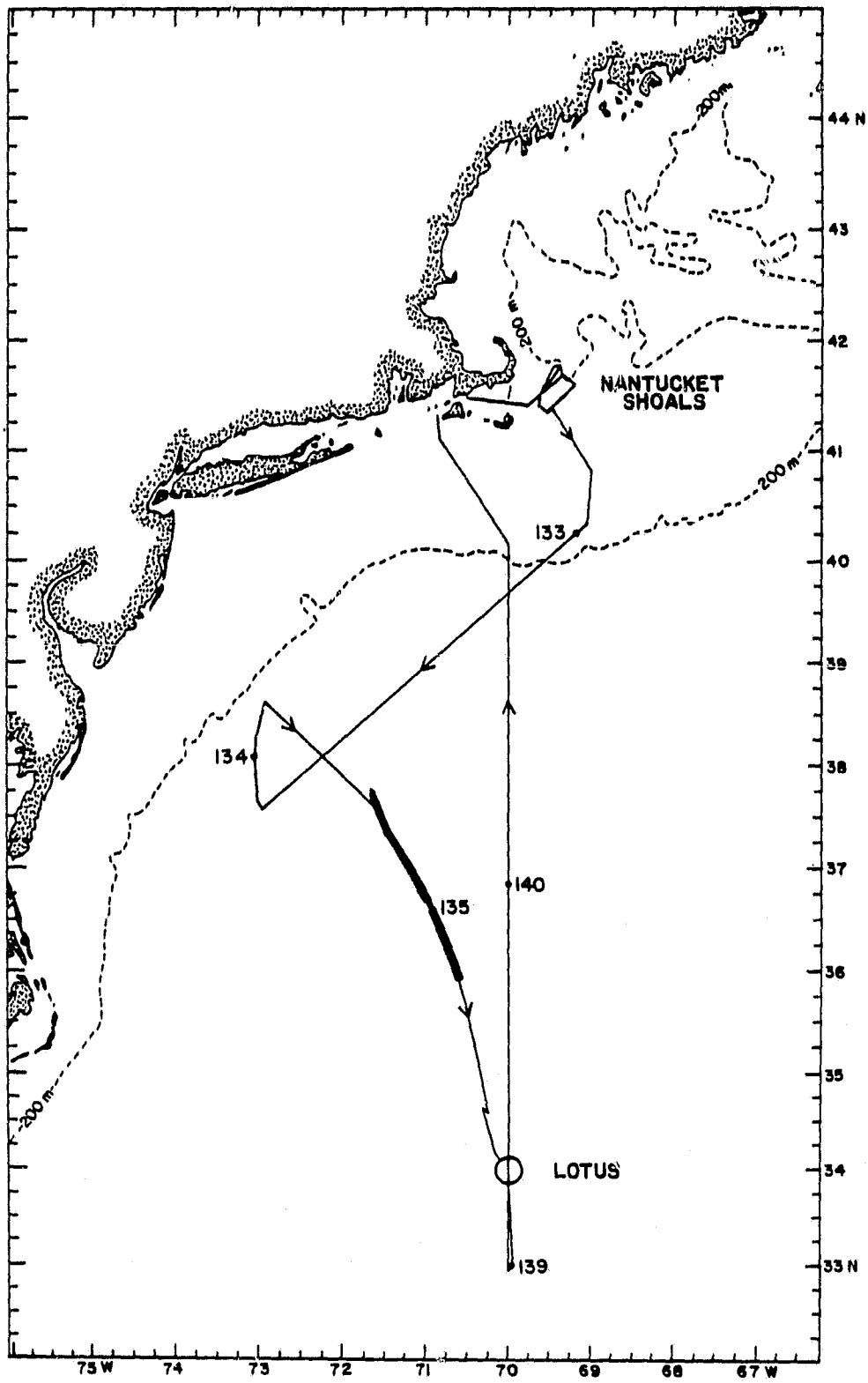

Figure 3: Ship track for R.V. OCEANUS Cruise 96, 11 to 22 May. After day 132 (May 12) 1200Z position of vessel is plotted. Heavy lines indicate XBT and current profiler section across the Gulf Stream.

ORIGINAL PAGE IS
OF POOR QUALITY

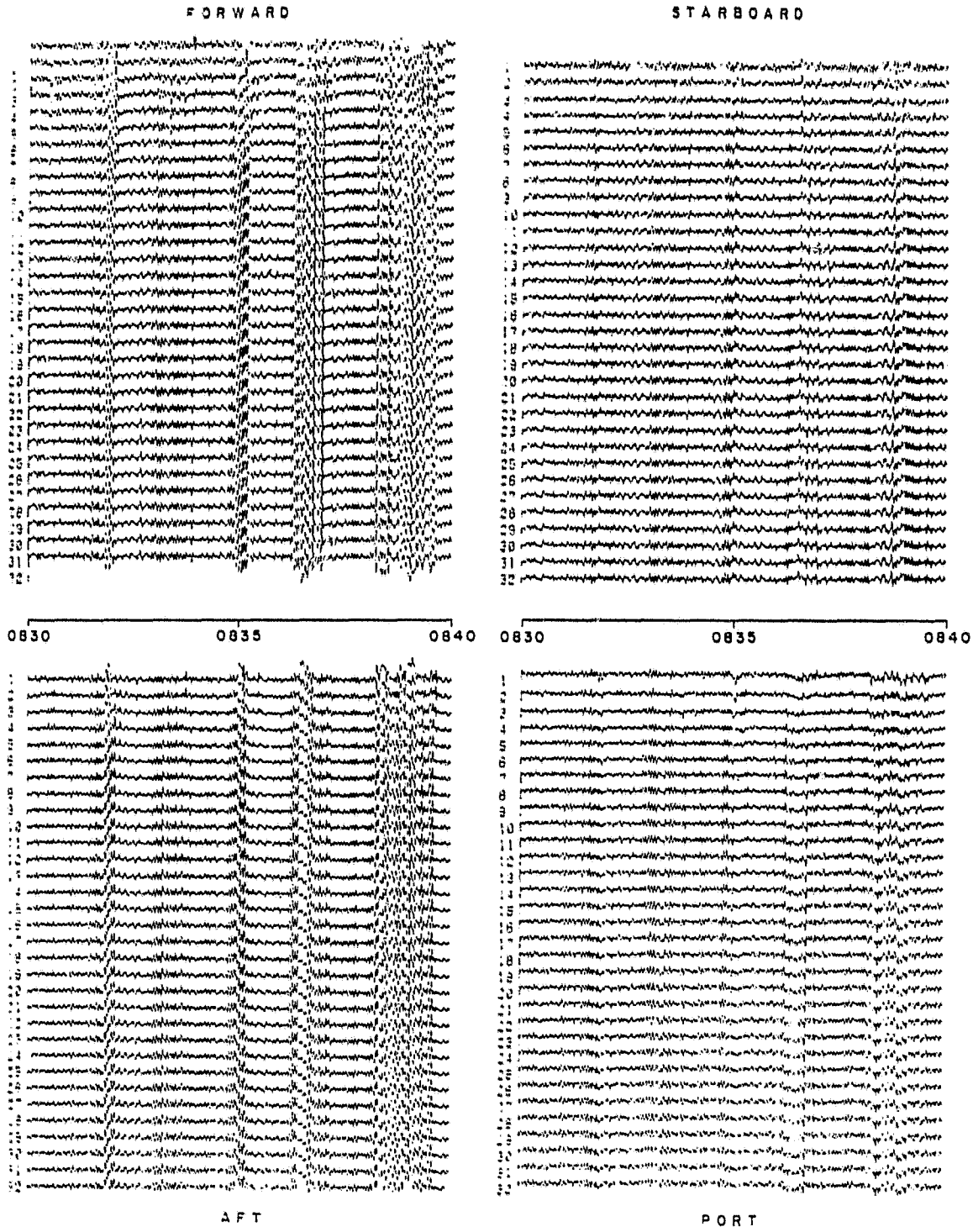

Figure 4: Raw Doppler counts for four acoustic beams during a 10-minute period 0830-0840Z on day 135. An 1800-Hz range in the Doppler frequencies in the forward beam is used to scale the returns from each of the four beams.

ORIGINAL PAGE IS
OF POOR QUALITY

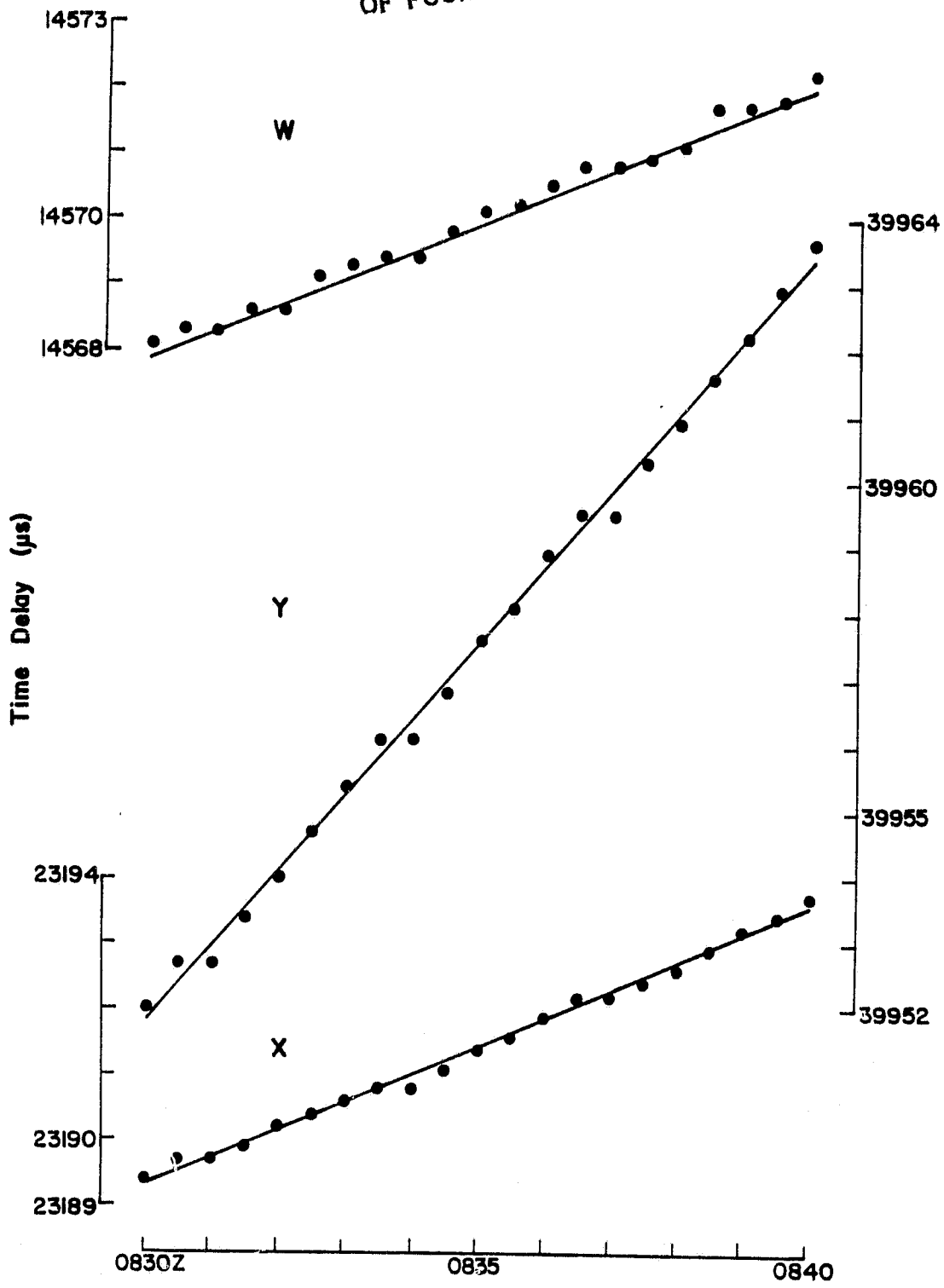

Figure 5: Ten-minute series of time delays showing 30-s sampling for three stations in the northeast U.S. chain (9960) with least-square fits to a bias and slope for each time delay series.

ORIGINAL PAGE IS
OF POOR QUALITY

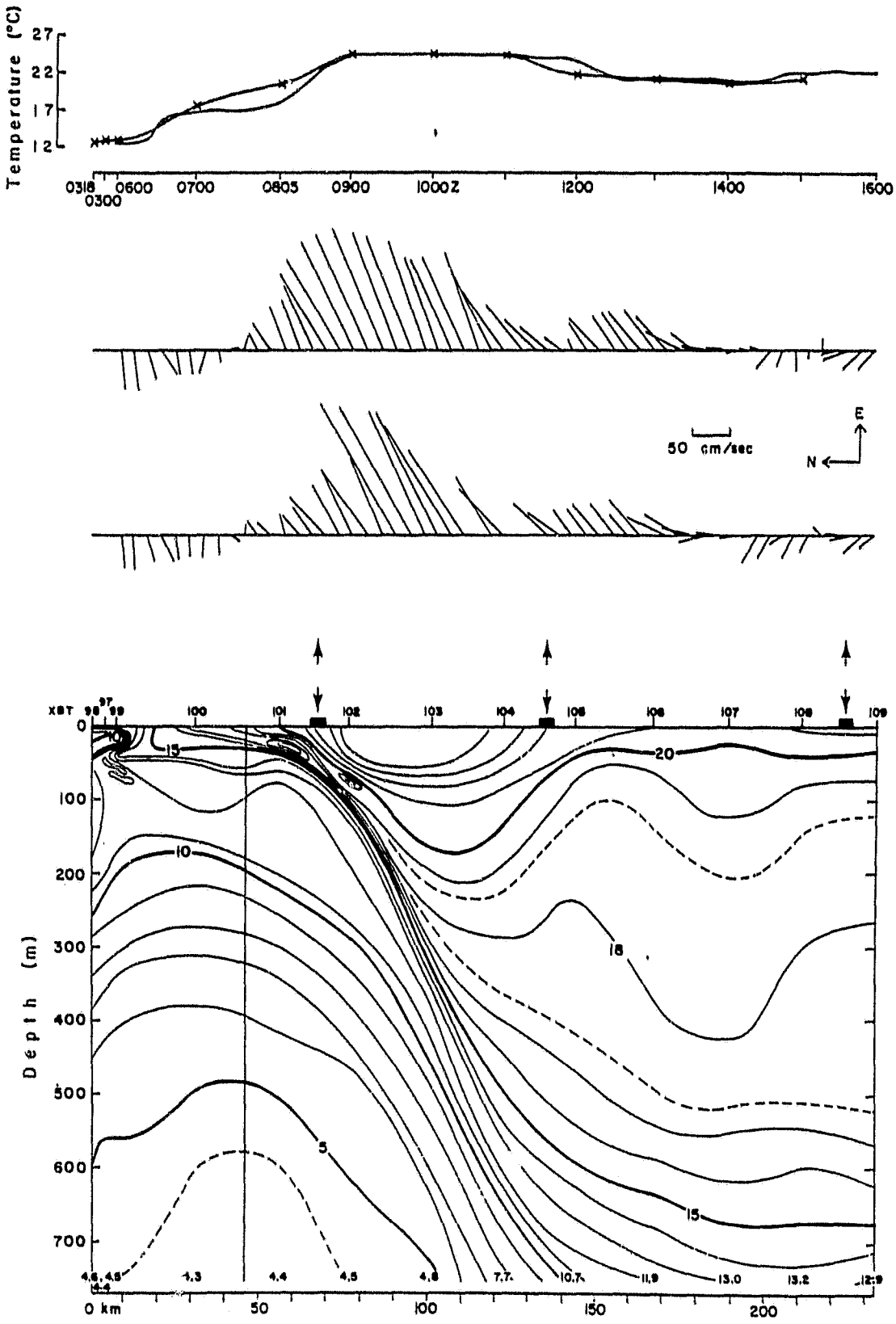

Figure 6: Section across the Gulf Stream showing bucket (X) and thermistor temperatures (note the 30-minute lag of the thermistor), upper panel: vector-averaged currents at depths of 28 and 99 m (second and third panels, respectively); XBT section with XBT numbers and three 10-minute segments selected for current profiles and denoted by arrows.

ORIGINAL PAGE IS
OF POOR QUALITY

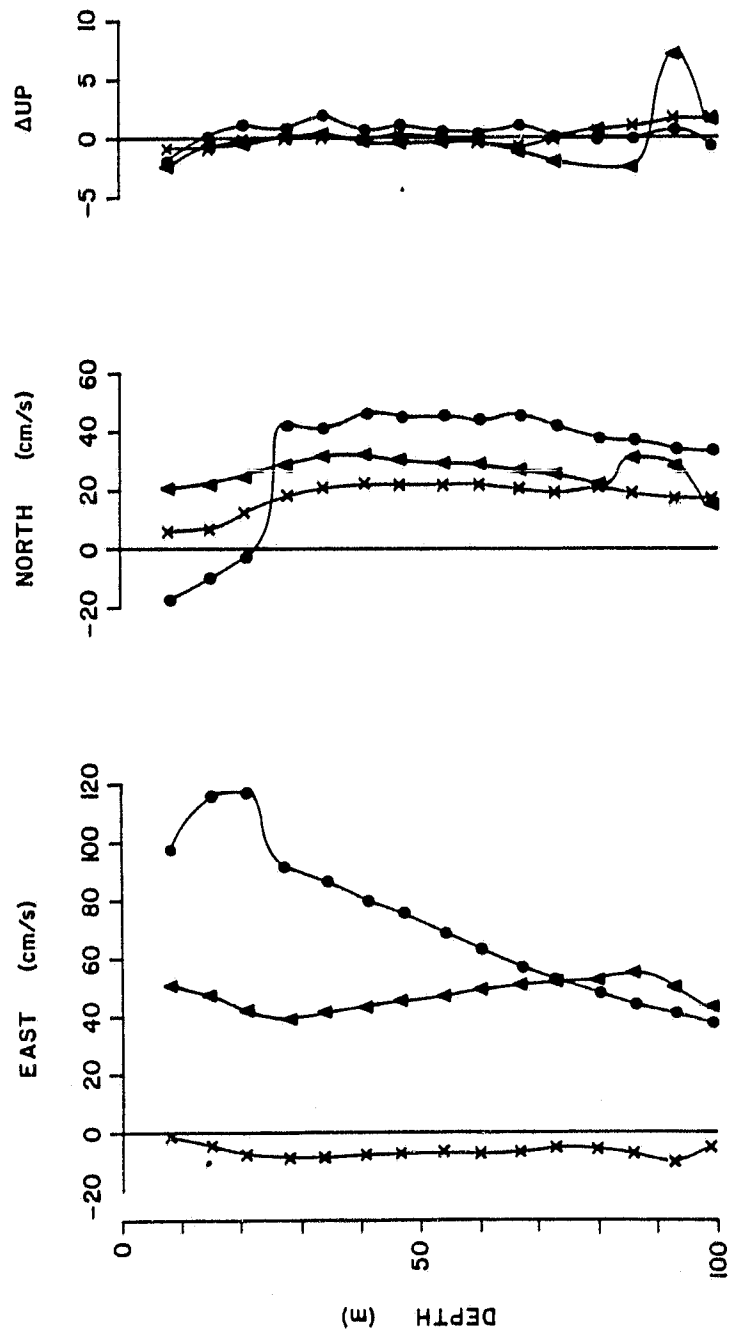

Figure 7: Vector-averaged horizontal velocities for the three 10-minute time intervals shown in Figure 6 from the Gulf Stream north wall (●), south wall (▲), and Sargasso Sea (X). Difference between two vertical velocity estimates is plotted at the right on an expanded scale. Only data judged 'good' by Ametek-Straza interface cards were used. The large shear at 20 m in the north wall profile is across the base of the mixed layer and could be due to inertial waves.

ORIGINAL PAGE IS
OF POOR QUALITY

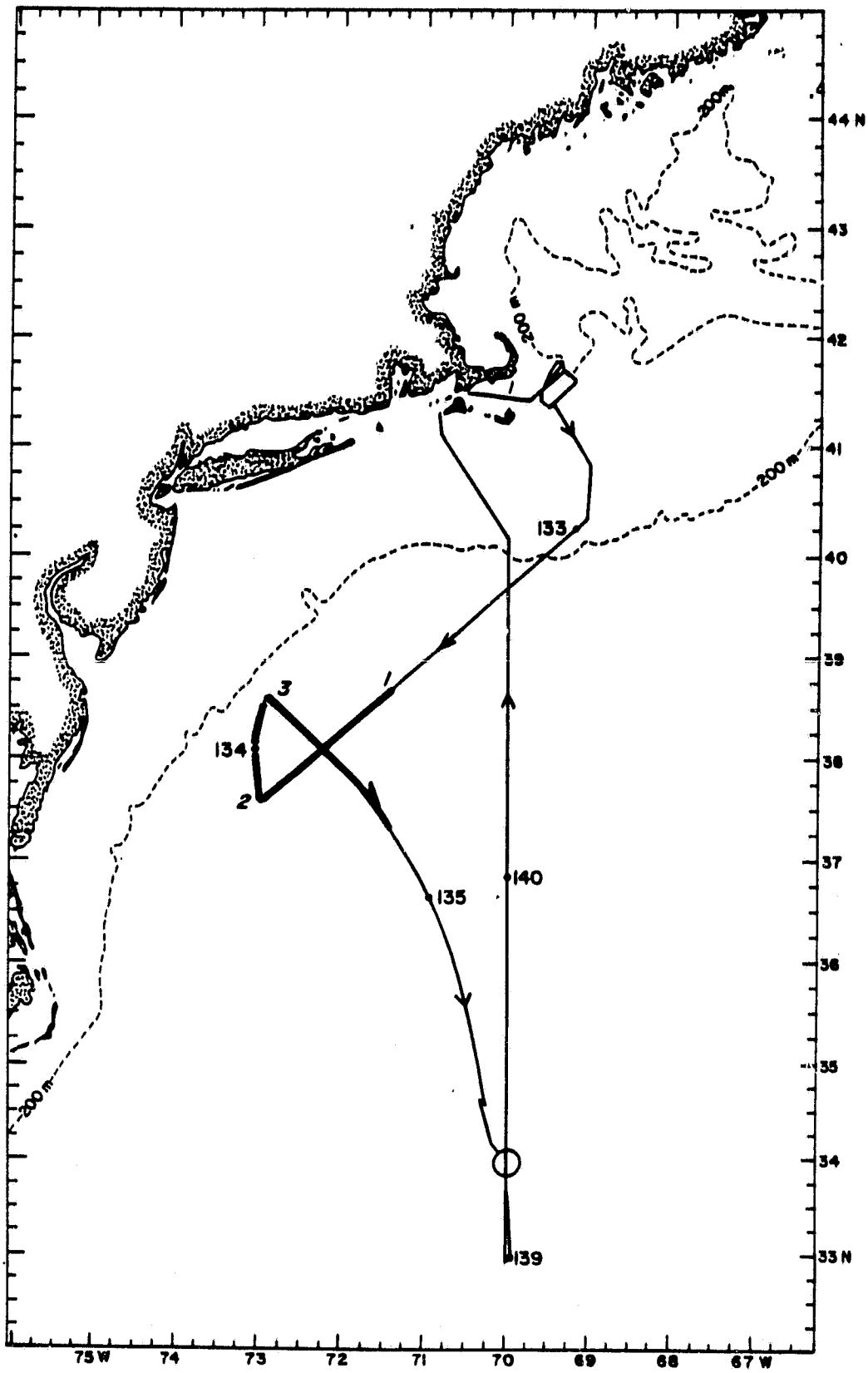

Figure 8: Ship track for R.V. OCEANUS Cruise 96. Heavy line shows three XBT and current profiler sections through a Warm Core Gulf Stream Ring. The numbers identify each of the three sections.

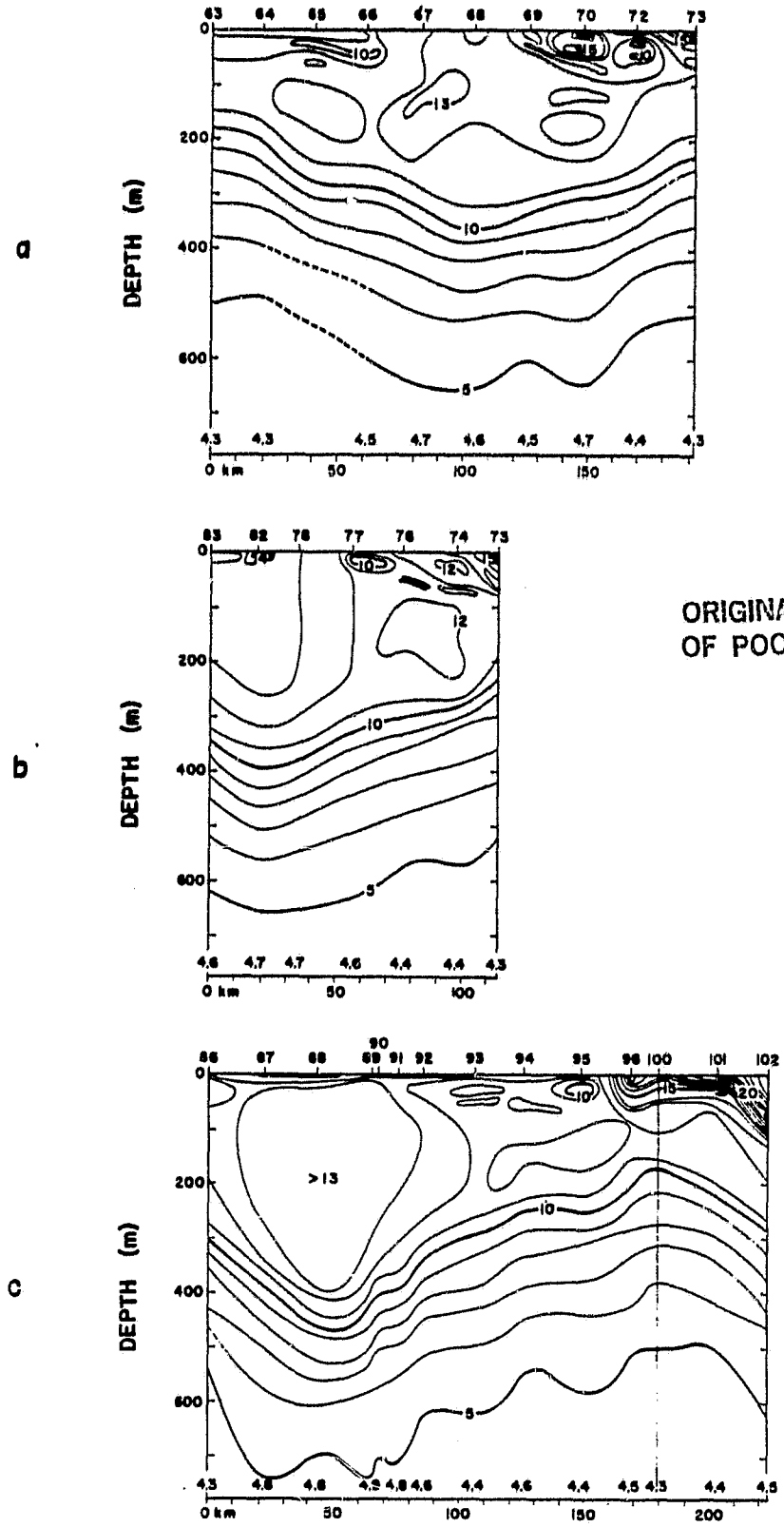

Figure 9: Temperature profiles obtained from three XBT sections through the WCR. As numbered in Figure 8, Leg 1 is the upper panel (a), Leg 2 the second panel (b), Leg 3 the lower panel (c). All profiles are plotted as if the observer were locking from west to east. Numbers on the upper edge of each figure refer to XBT numbers; those on lower edge give temperatures at 760 m. Steep dipping of the isotherms at Stations 101 and 102 shows the beginning of the cold wall.

ORIGINAL PAGE IS
OF POOR QUALITY

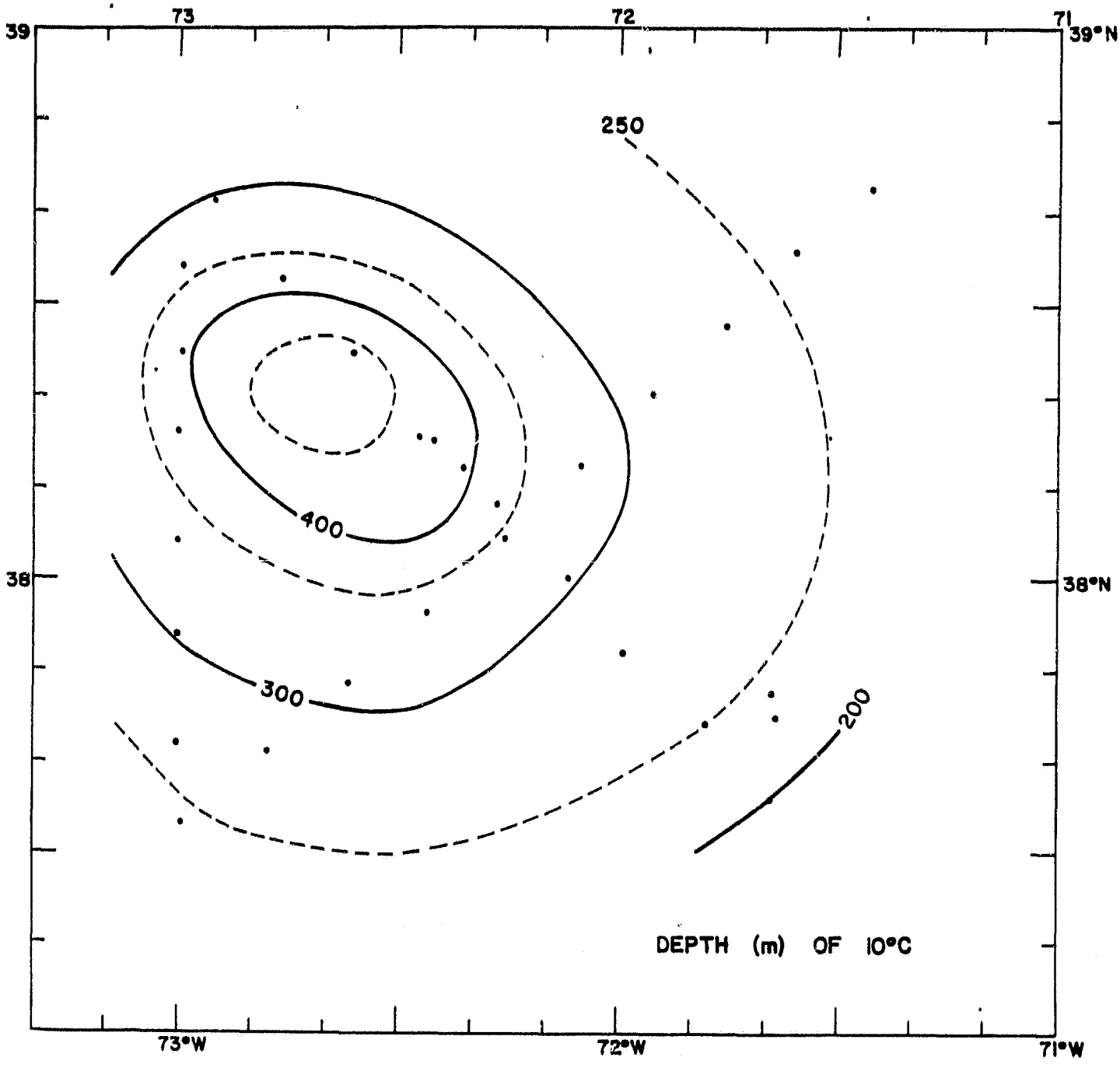

Figure 10a: The depth of the 10°C isotherm from XBT data showing the position of the ring center.

ORIGINAL PAGE IS
OF POOR QUALITY

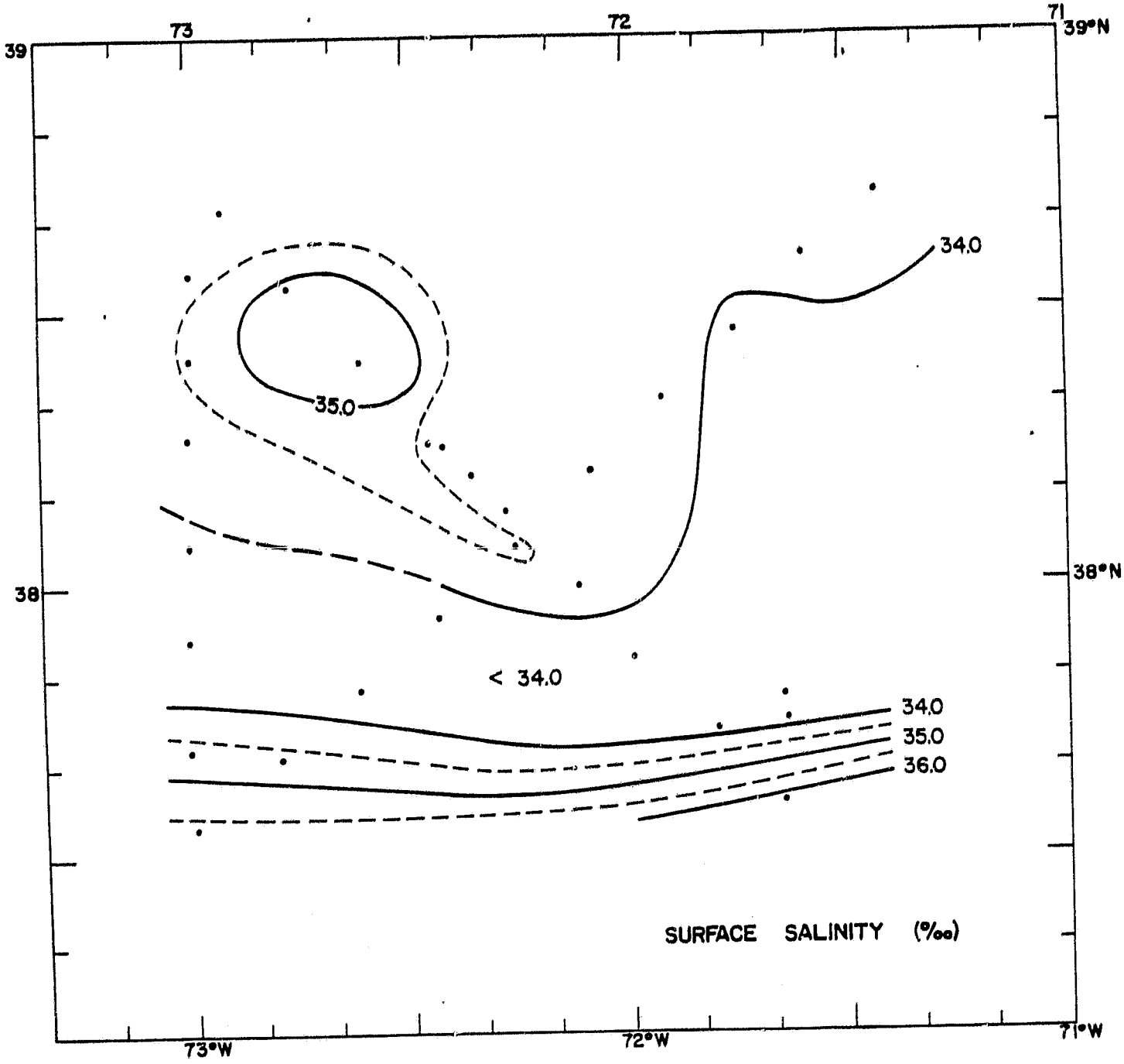

Figure 10b: Contour of surface salinities in the WCR from bucket samples at each XBT. Sharply increasing salinities south of the ring show the edge of the Gulf Stream.

ORIGINAL PAGE IS
OF POOR QUALITY

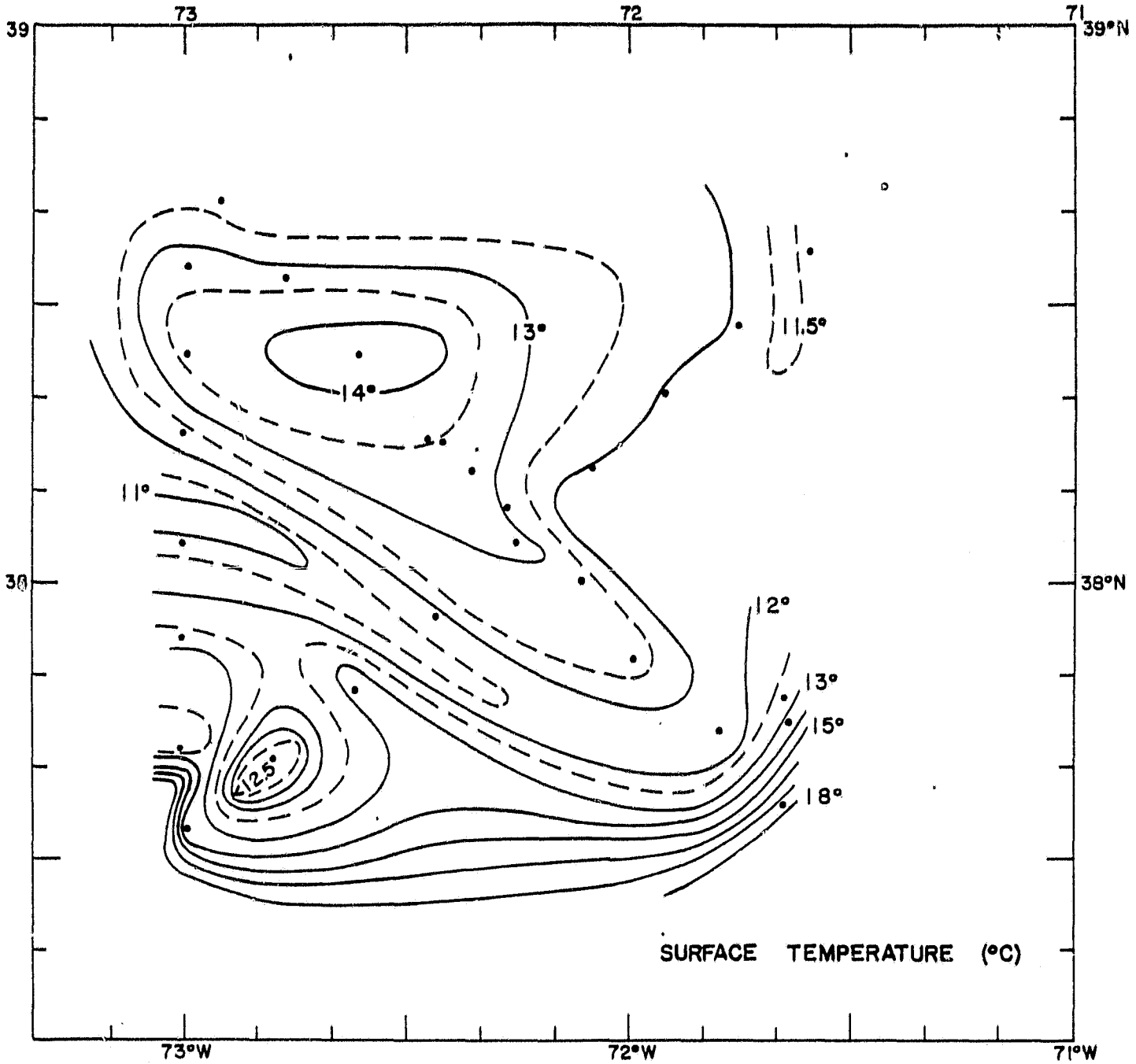

Figure 10c: Contour of sea surface temperatures recorded by thermistor during ring crossing. Warm (15°-18°C) water at the SE and SW ends of the X-pattern shows the ship reached the cold wall of the Gulf Stream.

ORIGINAL PAGE IS
OF POOR QUALITY.

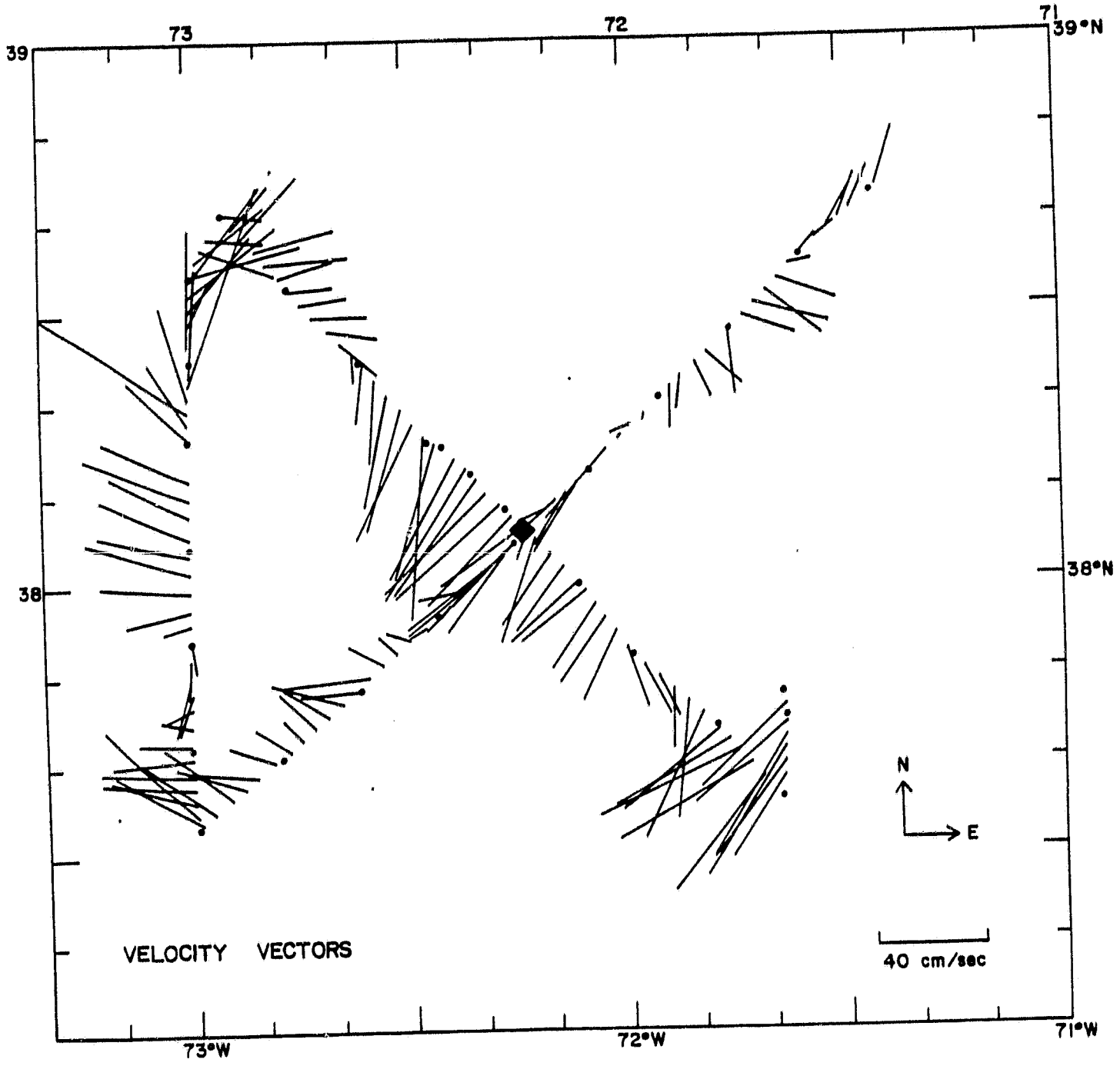

Figure 10d: Velocity vectors at 28 m depth in WCR calculated from 10-minute averages of the Doppler-velocimeter measurements. (◆) indicates 10-minute segment selected for current profile in Figure 11.

ORIGINAL PAGE IS
OF POOR QUALITY

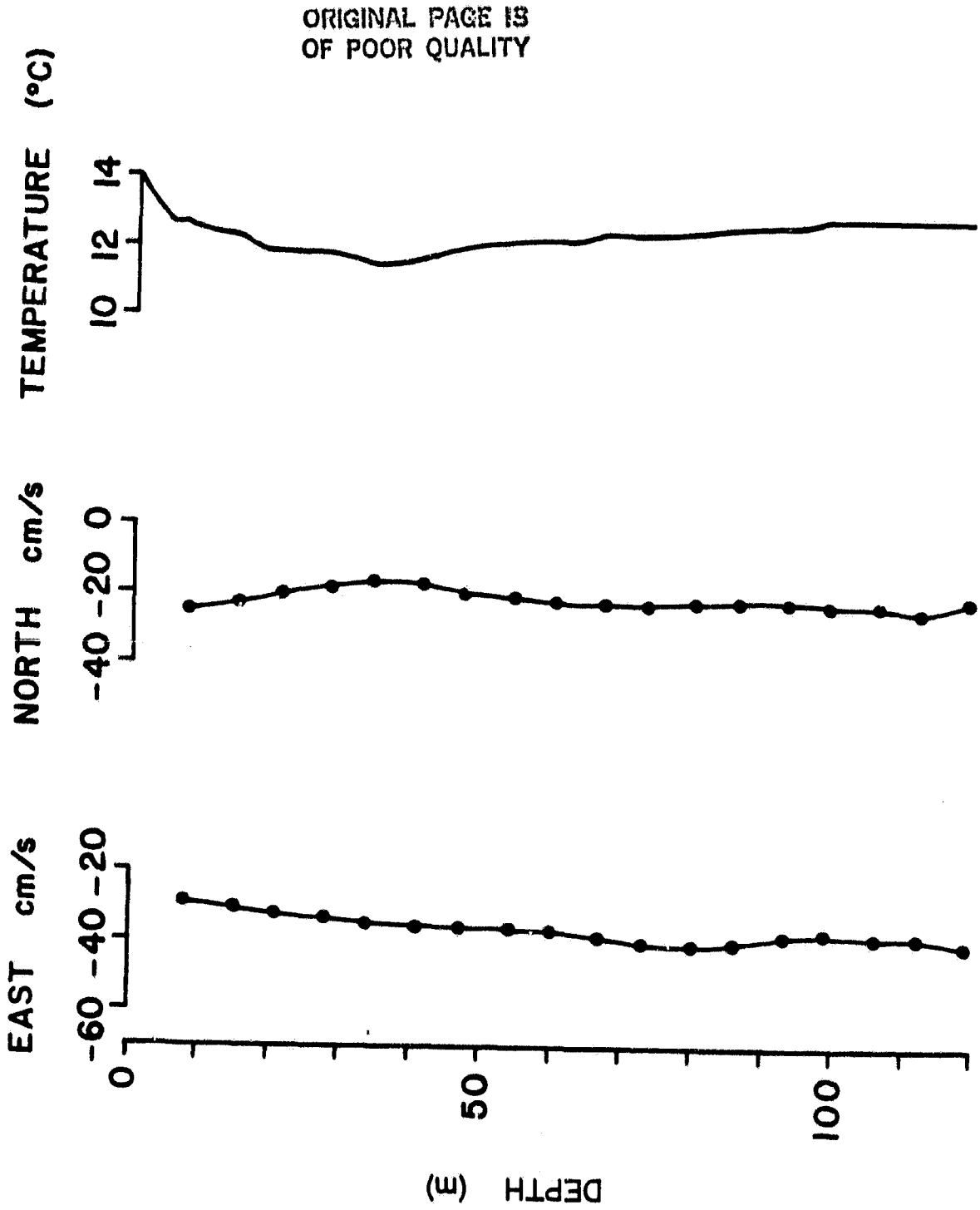

Figure 11: Vector-averaged horizontal velocities and temperature profile for 10-minute interval shown in Figure 10d. (Current record average begins at 2216 of day 134; temperature data from XBT 92, at 2200 of day 134.) Location of this profile is shown by the (◆) in the previous figure.

ORIGINAL PAGE IS
OF POOR QUALITY

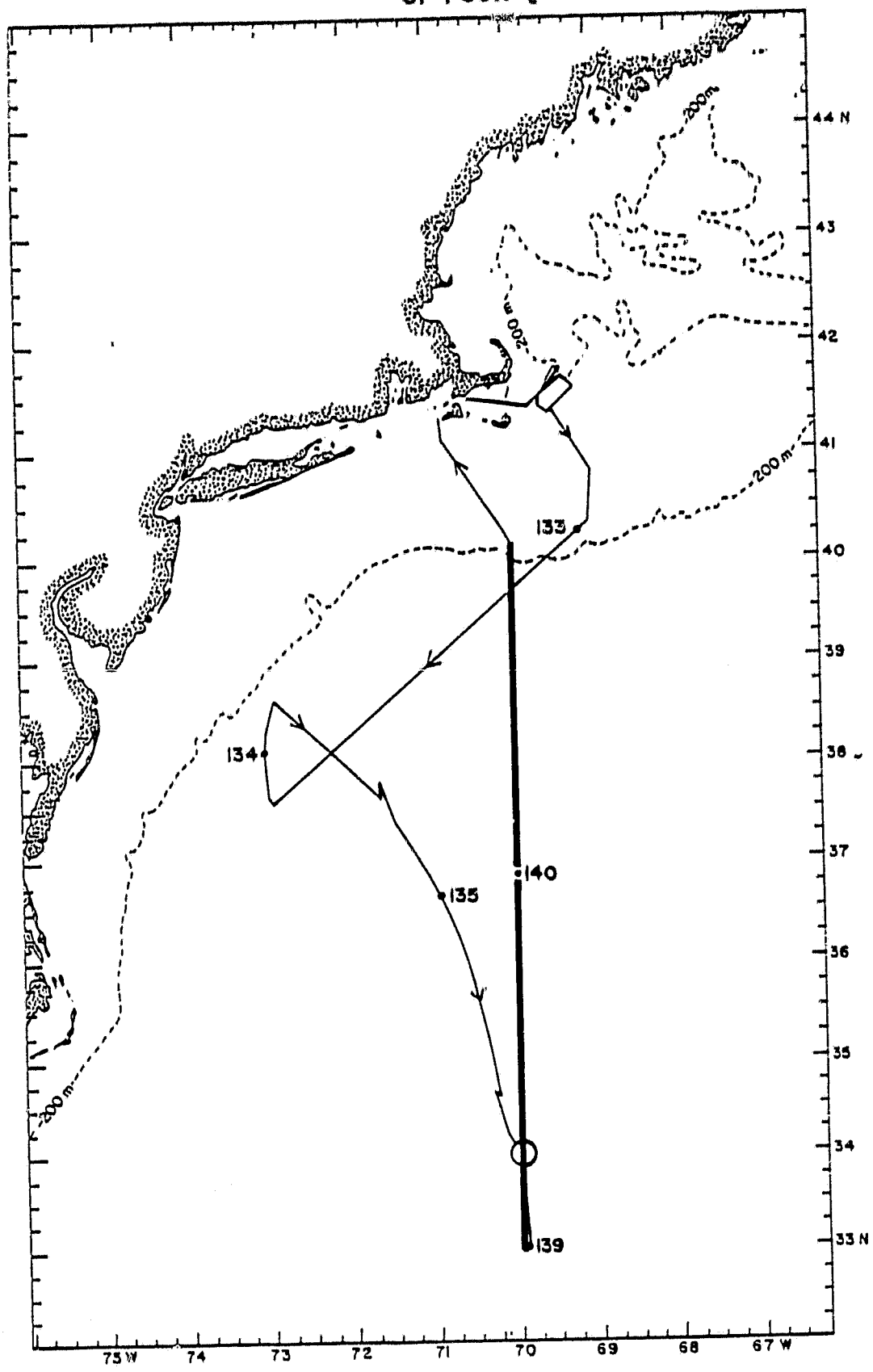

Figure 12: Ship track for R.V. OCEANUS Cruise 96. Heavy line denotes XBT and current profiler section along 70°W, from 33°N-40°N.

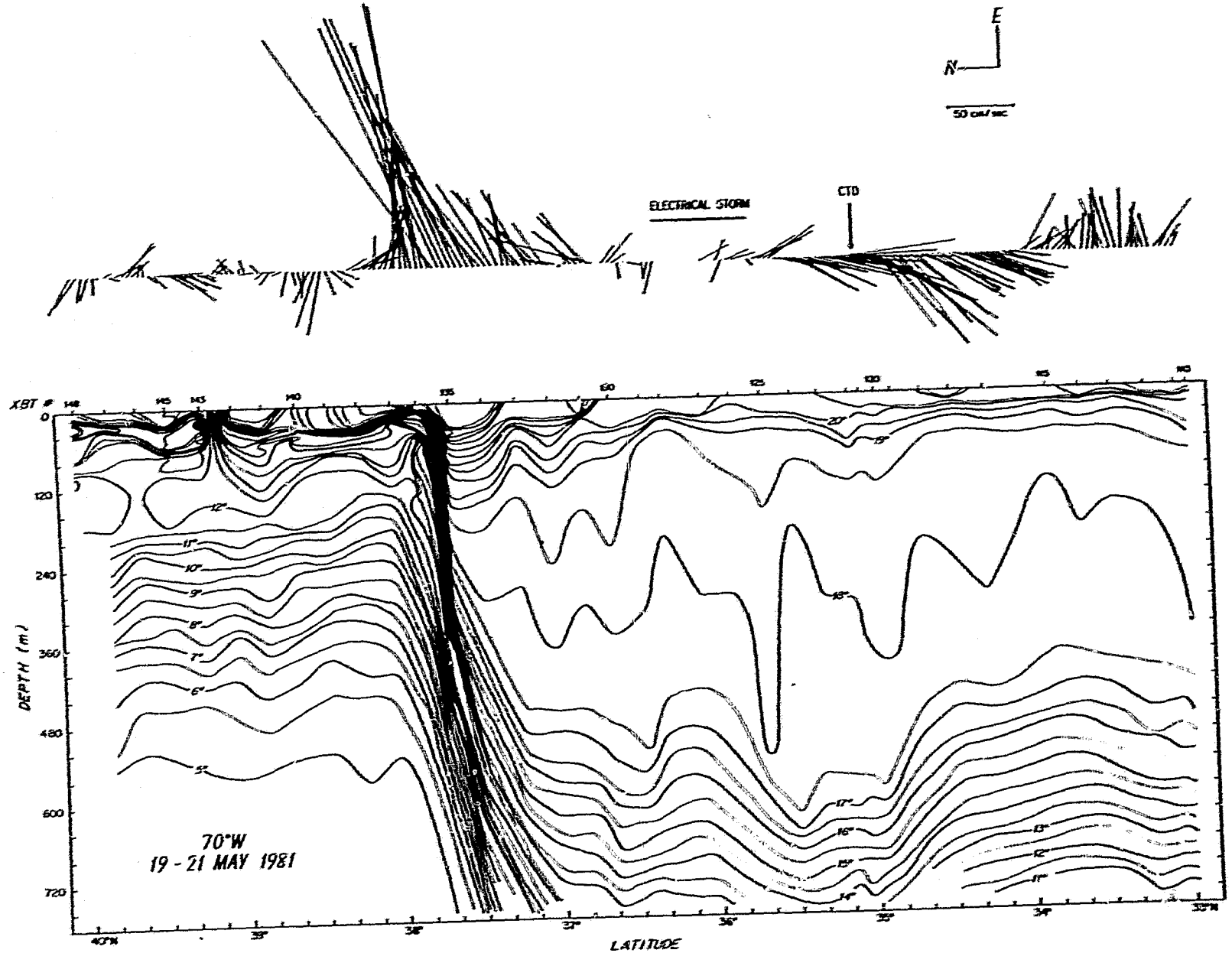

Figure 13: Section on 70°W showing vector-averaged currents at a depth of 28 m and XBT section with XBT numbers on the upper edge. (Electrical storm from 36°N to 37°N prevented accurate knowledge of ship motion, hence no velocity vectors could be calculated.)

ORIGINAL PAGE IS
OF POOR QUALITY

ORIGINAL PAGE IS
OF POOR QUALITY

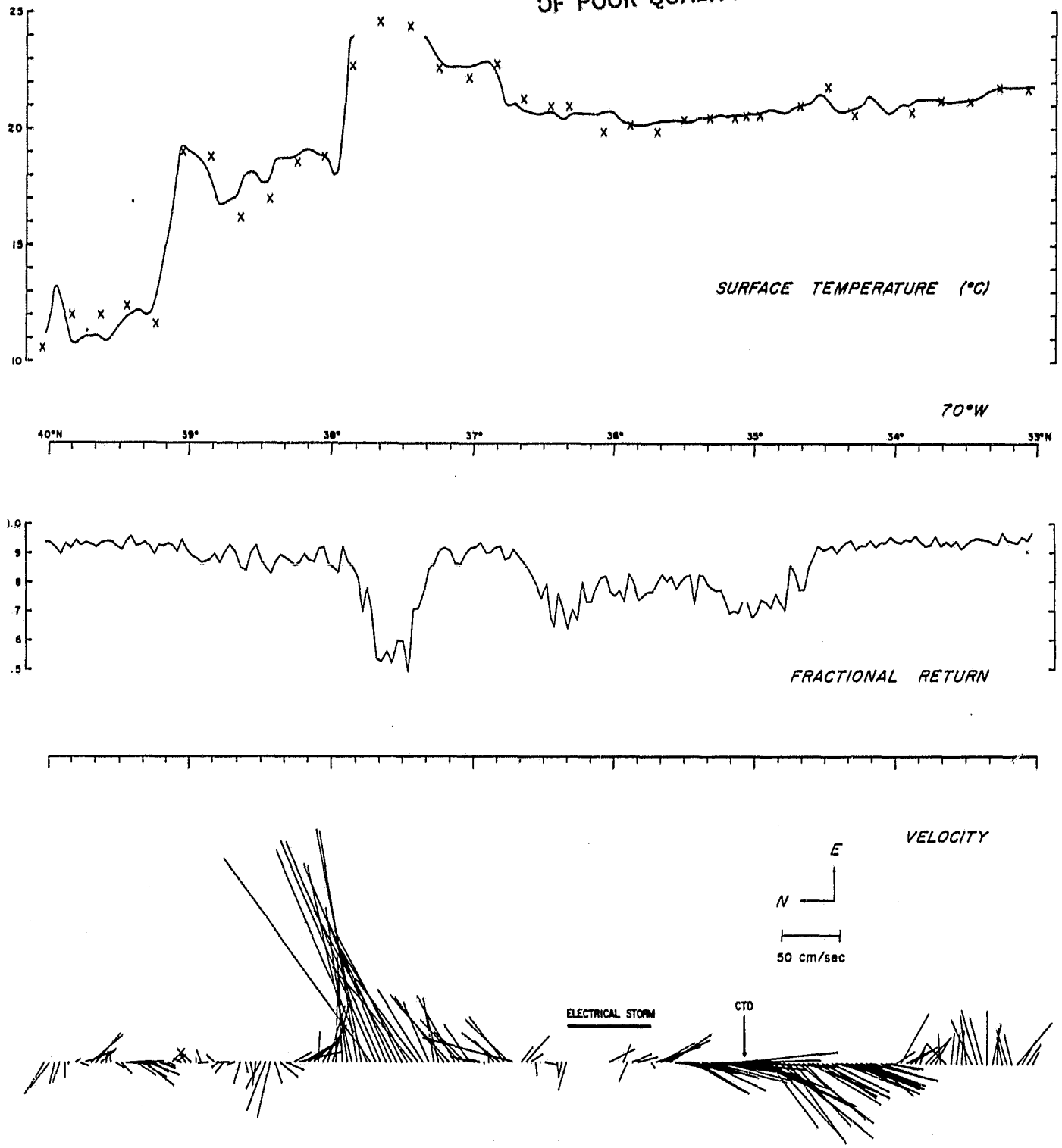

Figure 14: Contour of surface temperature on 70°W section measured by thermistor (solid line) and XBT (X), upper panel; strength of return signal at 28 m expressed as fractional return, second panel. Velocity vectors at 28 m from Figure 13 are included in lower panel for comparison.

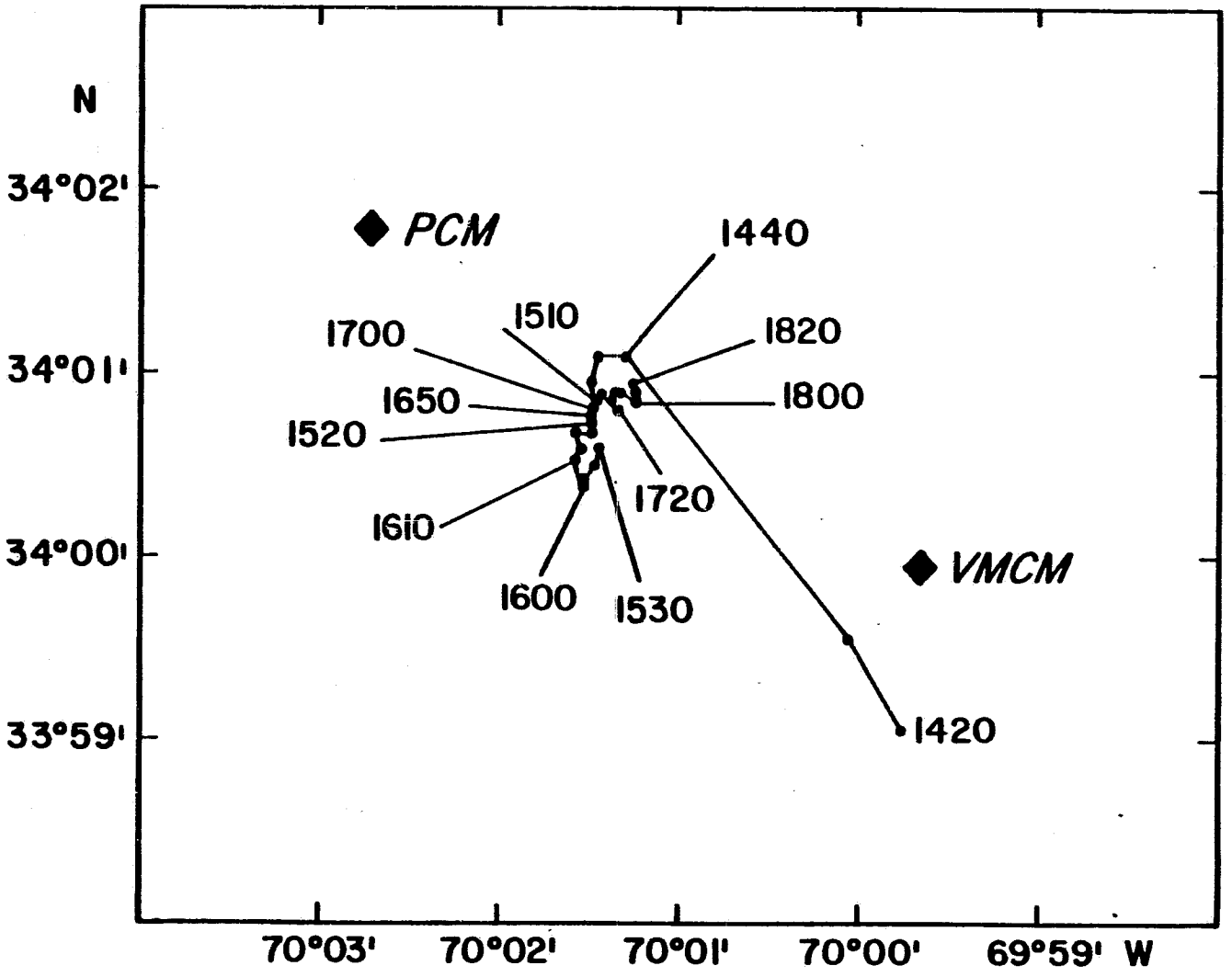

Figure 15: Ship track during intercomparison of current meters at the LOTUS site (see Figure 3). The position of the profiling current meter (PCM) and vector measuring current meter (VMCM) is indicated.

ORIGINAL PAGE IS OF POOR QUALITY

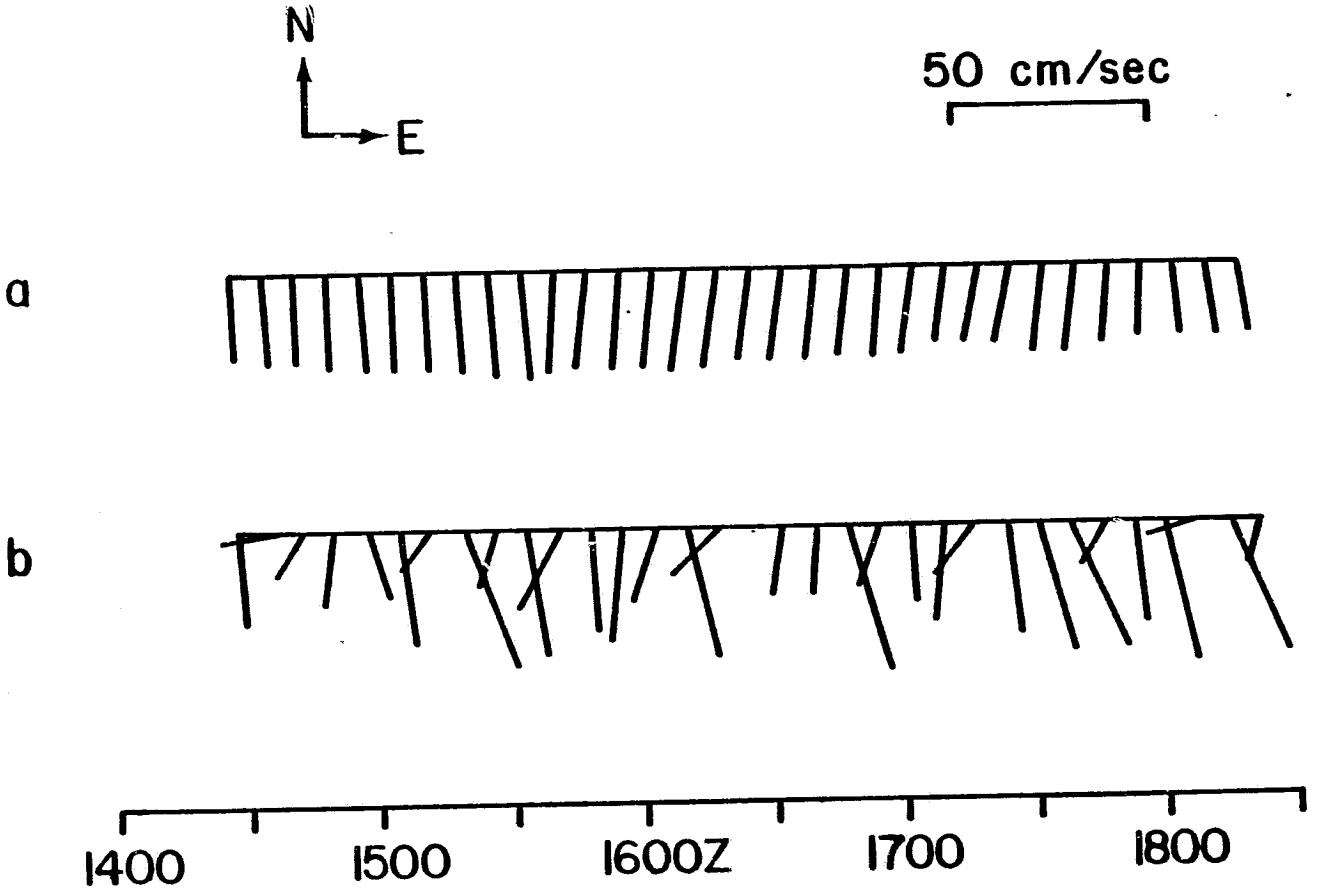

Figure 16: Time series comparison of velocity vectors obtained from VMCM at 36 m (Figure 16a) and APOC at 34 m (Figure 16b). VMCM values are recorded every 7.5 minutes; APOC values are 7.5 minutes (fourteen record) vector averages. (Unequal spacing of APOC vectors results from rounding off to the nearest minute in the calculation for average time.

ORIGINAL PAGE IS
OF POOR QUALITY

ORIGINAL PAGE IS
OF POOR QUALITY

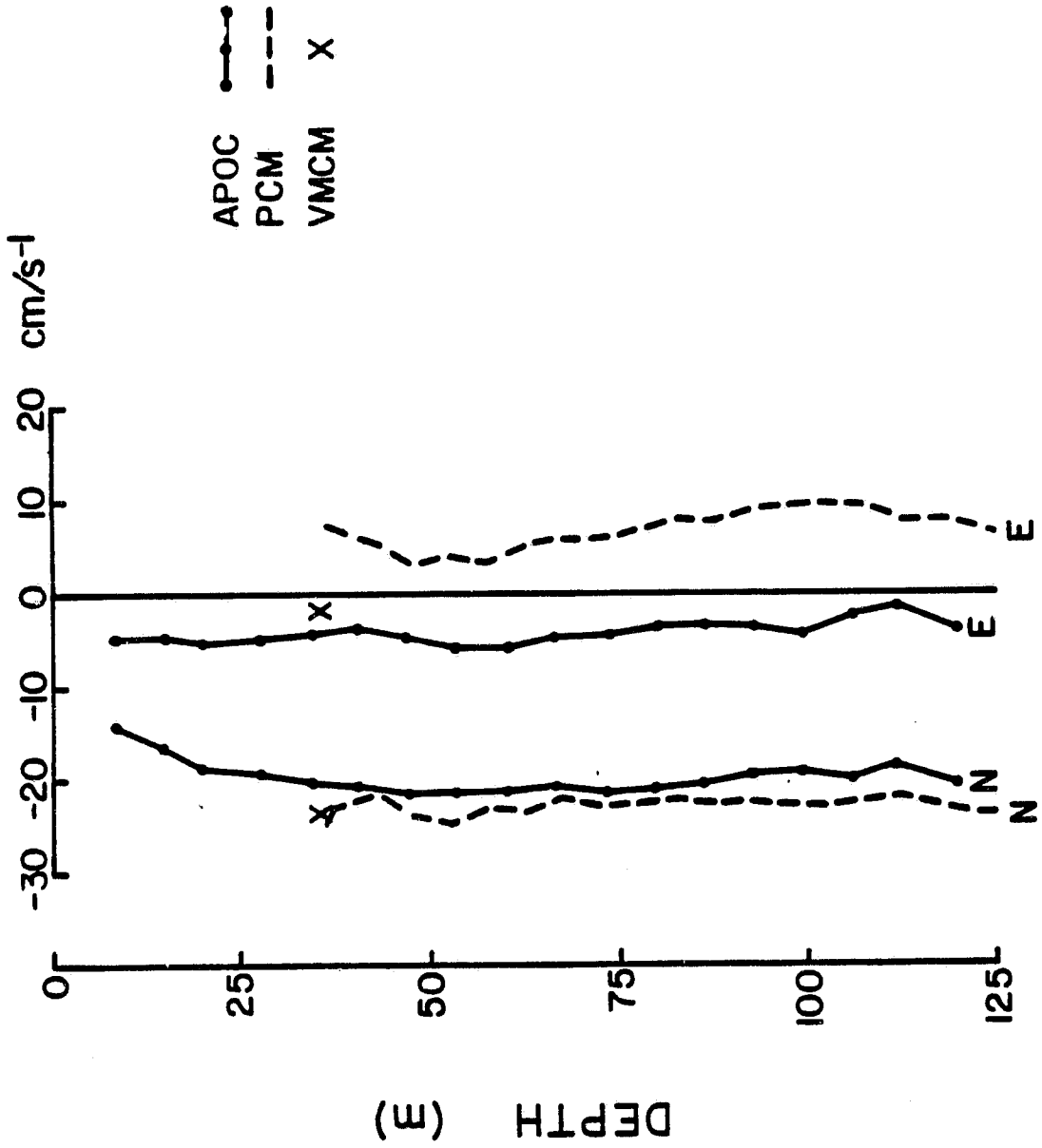

Figure 17: Comparison of N and E components of horizontal velocity as measured by APOC, PCM and VMCM at approximately 1615Z day 137. (APOC profile is vector average of measurements made at 1607, 1614, 1622 and 1636Z; PCM profile made at 1613Z; VMCM value is average of observations between 1607 and 1633Z.)

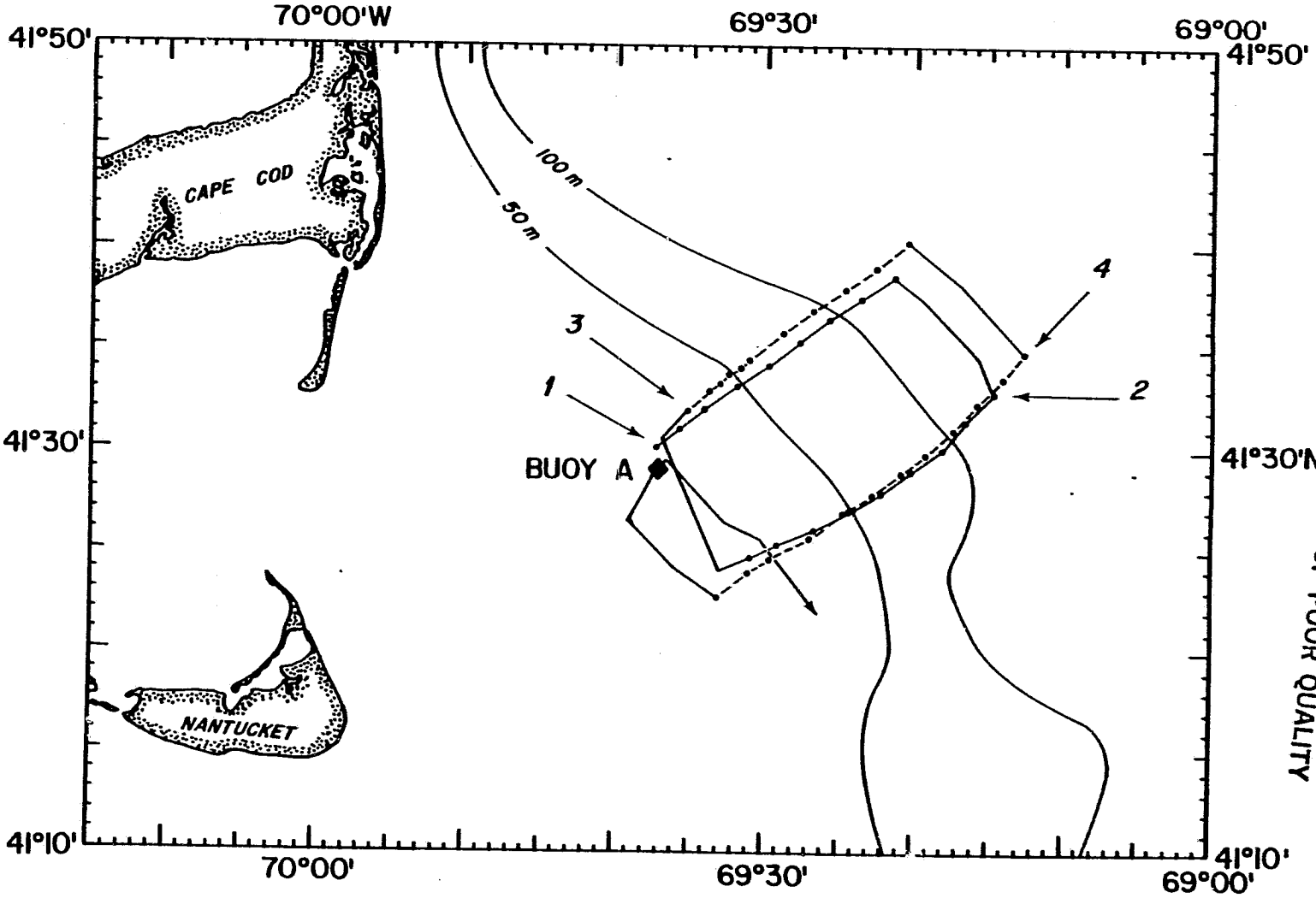

Figure 18: Ship track for 11-12 May, over Nantucket Shoals, showing XBT positions (see Figure 3). Sections are identified by number; during each Doppler velocimeter operated continuously. A time series plot of velocity vectors at Buoy A (◆) is found in Figure 19.

ORIGINAL PAGE IS
OF POOR QUALITY

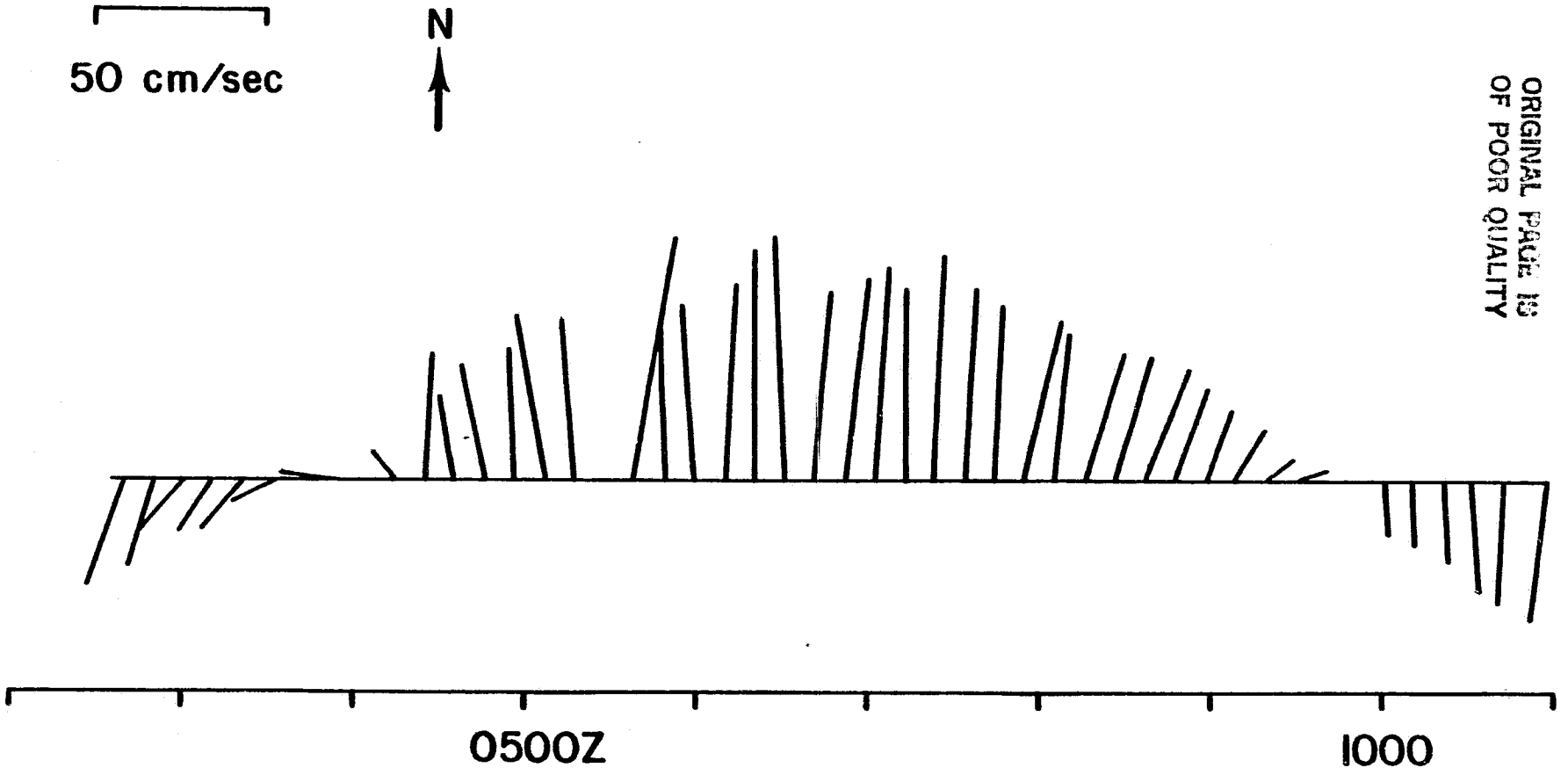

ORIGINAL PAGE IS
OF POOR QUALITY

Figure 19: Time series of 10-minute vector-averaged velocities at 20 m depth while on station at Buoy A (see Figure 18) from 0240-1100Z day 132.

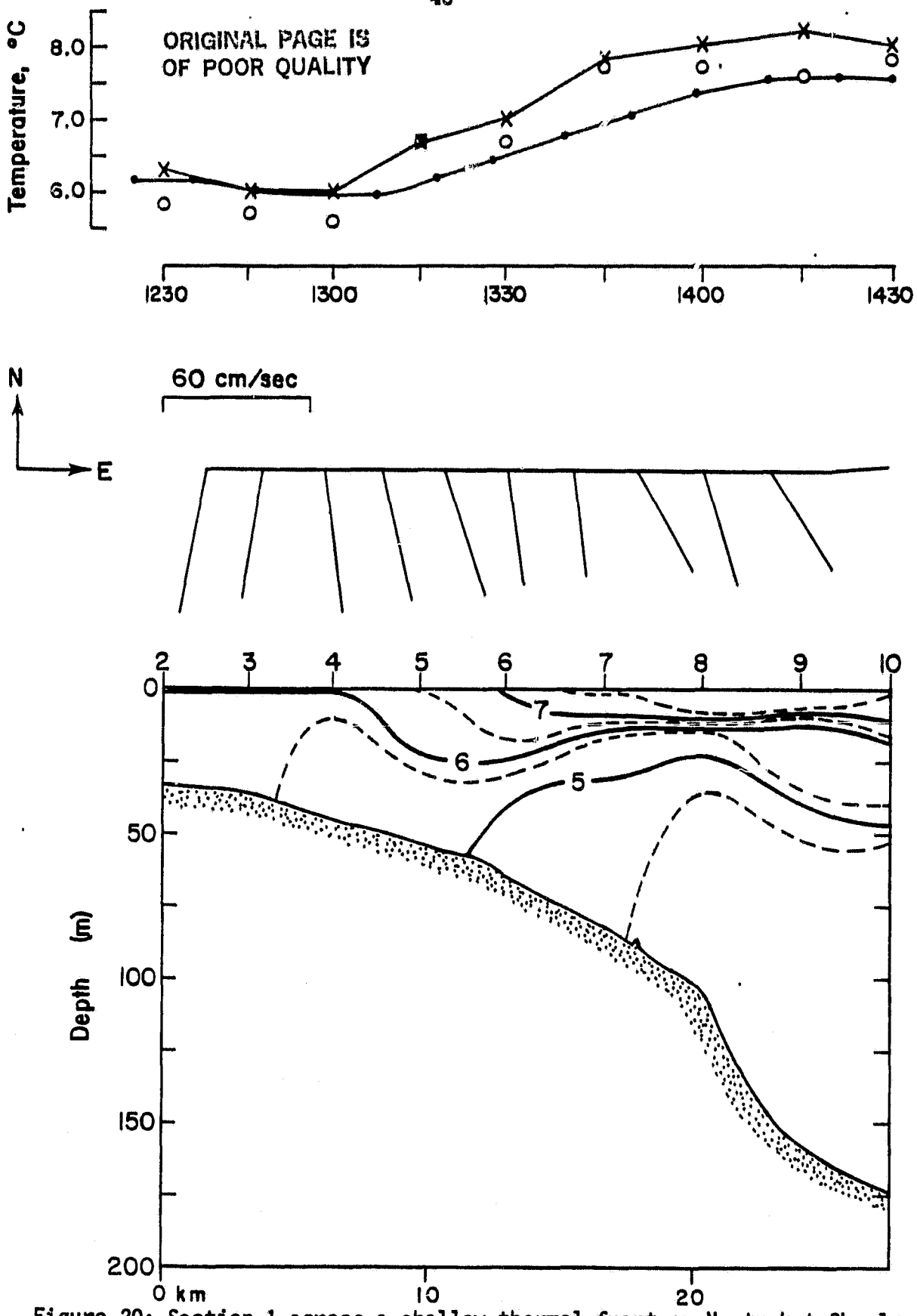

Figure 20: Section 1 across a shallow thermal front on Nantucket Shoals showing surface temperatures from bucket samples (X), XBT (O), and thermistor (•), upper panel; vector-averaged currents at 20 m depth, second panel; temperature profile constructed from XBT data, including bottom topography, lower panel. Dashed lines indicate half-degrees. Horizontal scale is the same in each figure.

ORIGINAL PAGE IS
OF POOR QUALITY

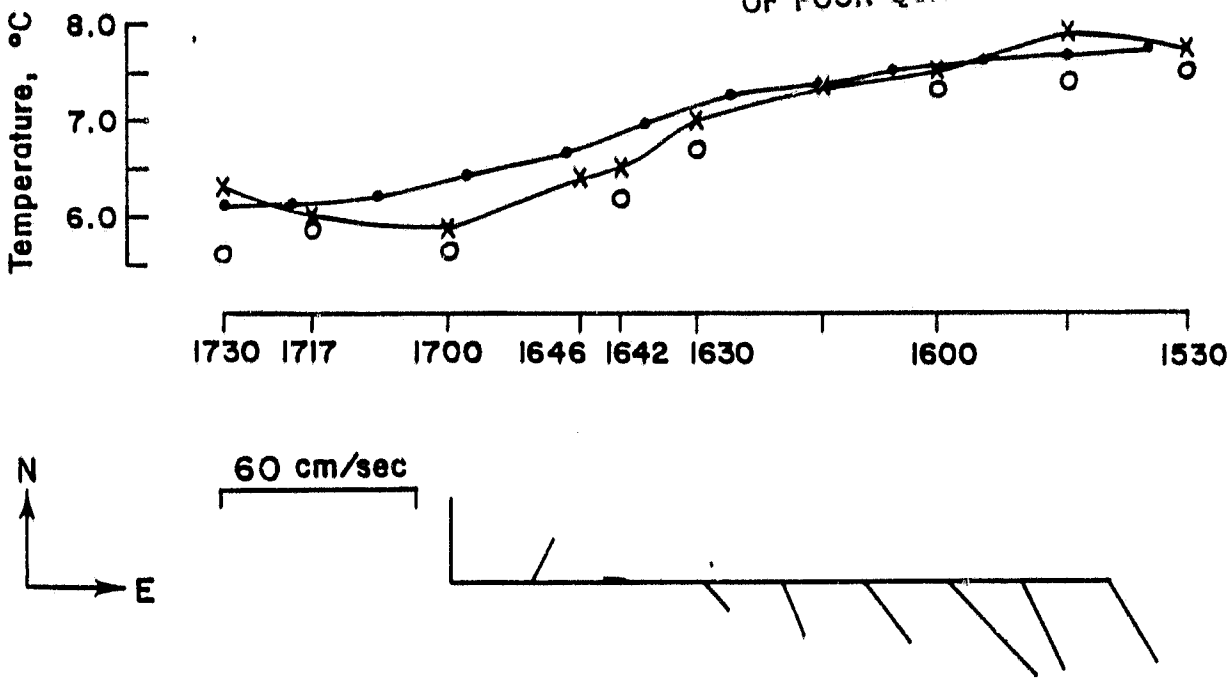

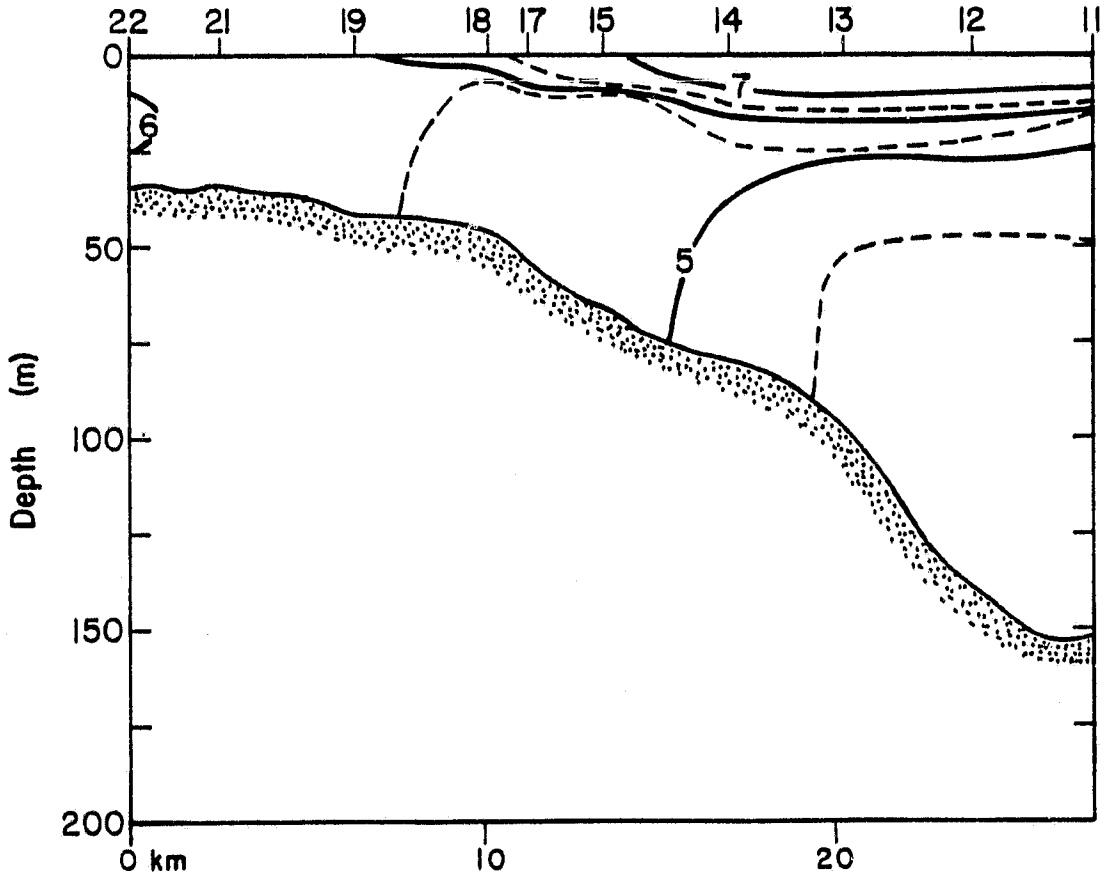

Figure 21: Same as Figure 20 for Section 2 (see Figure 18), 15 km to the SE.

ORIGINAL PAGE IS
OF POOR QUALITY

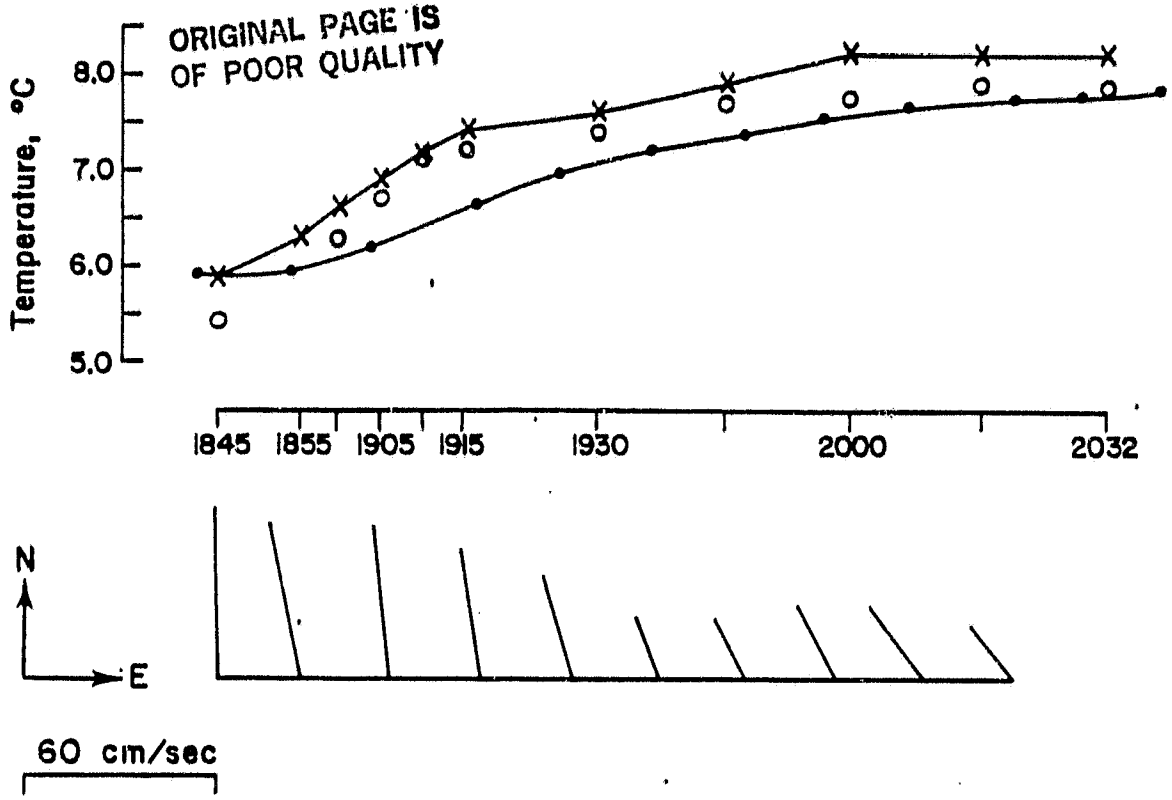

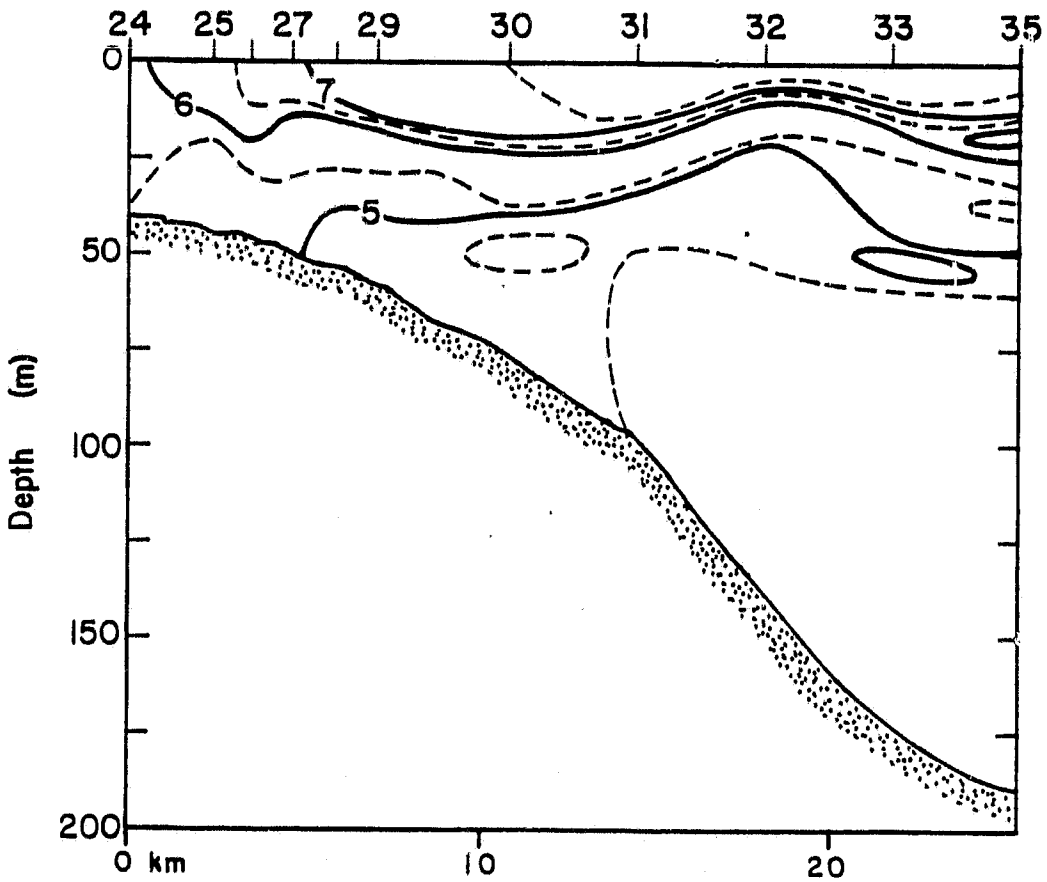

Figure 22: Same as Figure 20 for Section 3 (see Figure 18), repeating Section 1 six hours later.

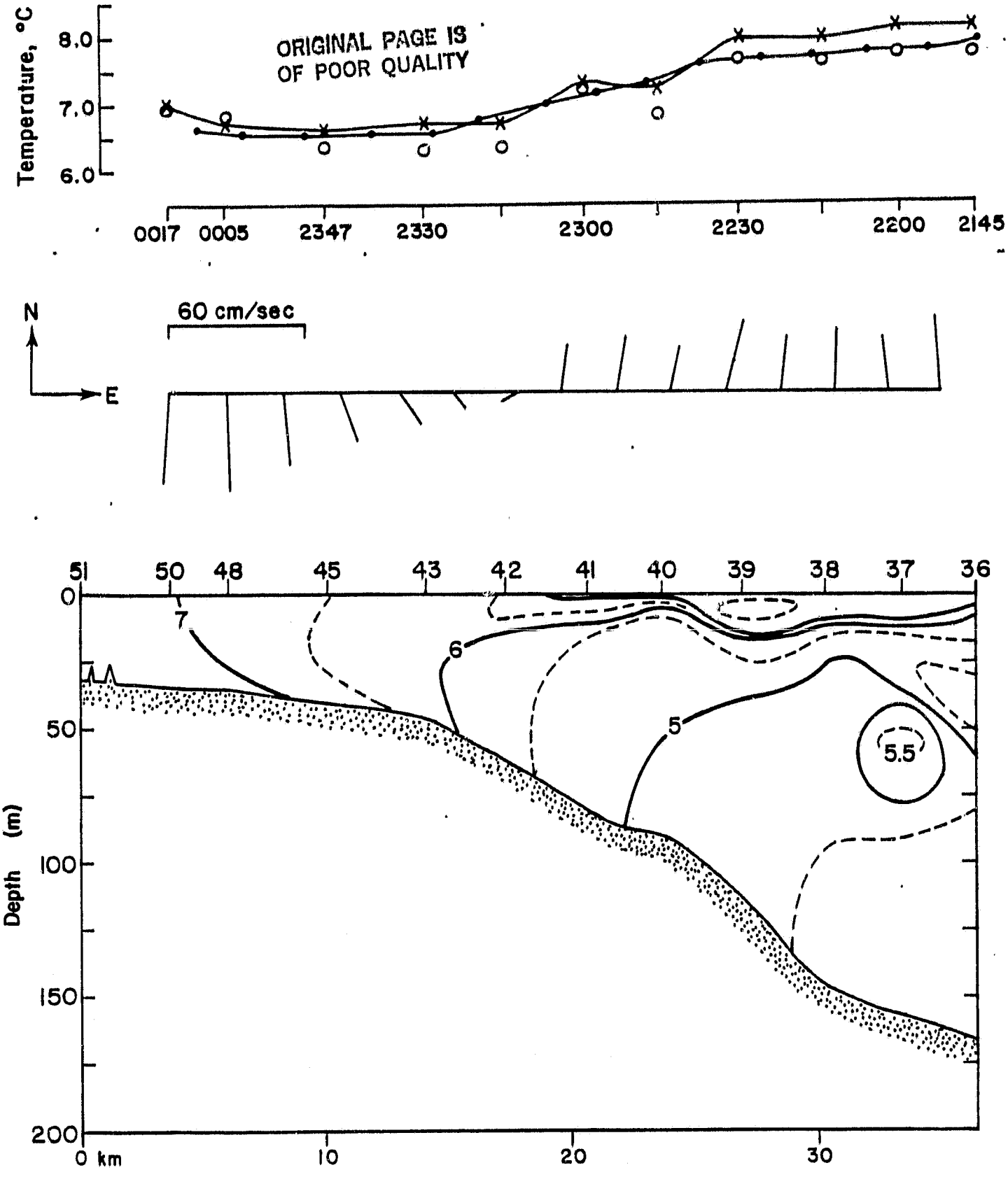

Figure 23: Same as Figure 20 for Section 4 (see Figure 18), which repeats Section 2 six hours later.

ORIGINAL PAGE IS
OF POOR QUALITY

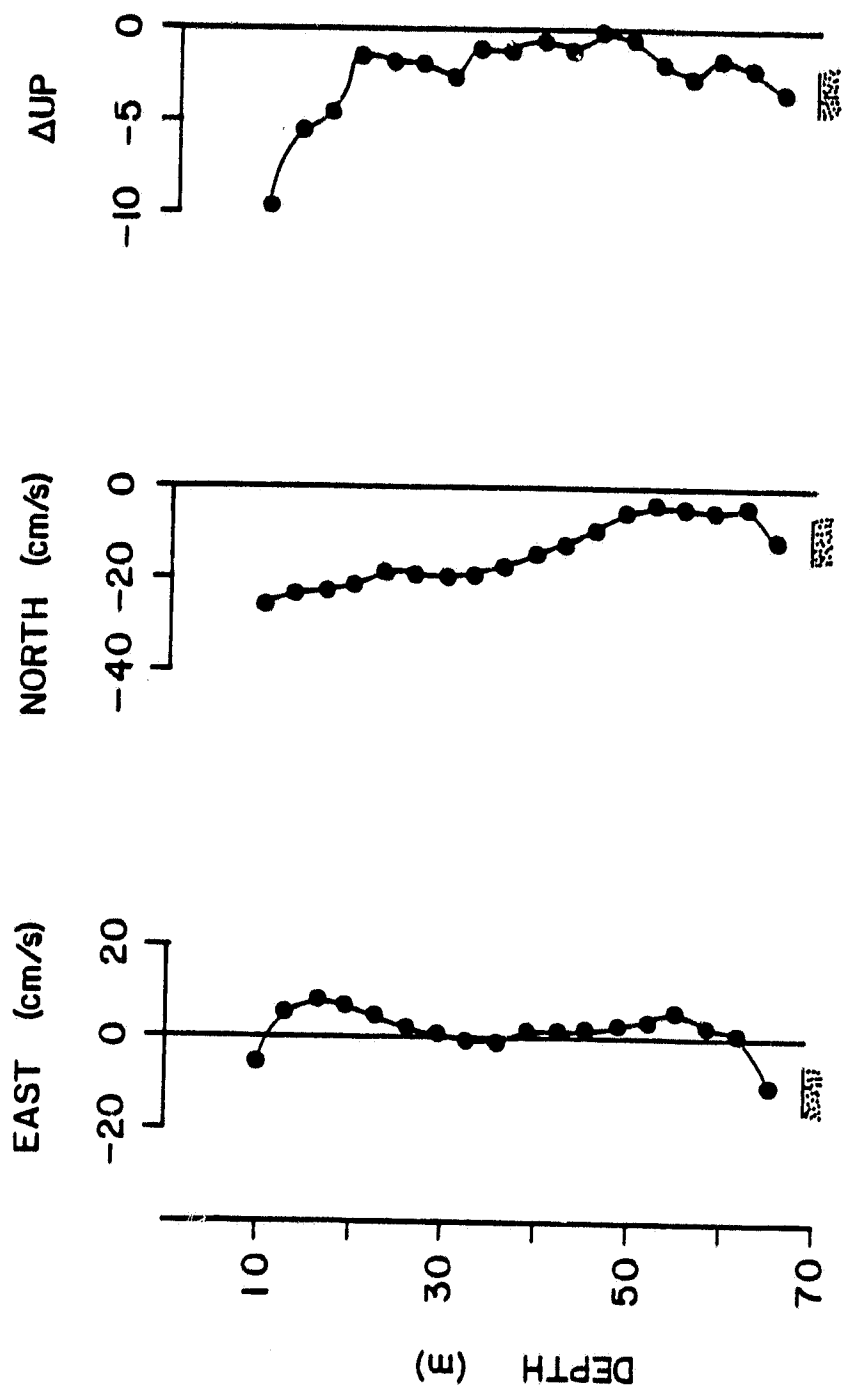

Figure 24: Vector averaged horizontal velocity profile for the 10-minute interval 1623Z (see Figure 21).